www.geocalcs.com/lap

LATERAL ANALYSIS OF PILES USER MANUAL

James P. Doherty

2020

james.doherty@uwa.edu.au

Version 2.0

Table of Contents

LIST OF TABLES

LIST OF FIGURES

GENERAL INFORMATION

LAP*:** (L***ateral ***A***nalysis of ***P***iles) is a web-based application for calculating the behaviour of vertical piles subjected to lateral loads.

Pile properties: The pile is modeled with structural beam elements and can be assigned either linear-elastic or elastic-perfectly plastic material properties. Up to ten different pile sections can be included in a single analysis.

Soil *p-y* curves: The soil is modeled as a collection of independent (*Winkler*) springs. The load-displacement behaviour of the springs can be specified using parameters for common *p-y* curves. Users can also specify their own *p-y* curves by pasting in tabulated data.

Loading: Pile loads can be specified as combination of horizontal forces, applied moments, prescribed horizontal displacements and prescribed rotations at any location along the pile. A surcharge load can be applied on the ground surface adjacent to the pile. This has the effect of increasing the total vertical stress in the soil by an amount equal to the value of the surcharge load.

Reaction springs: Horizontal and rotational reaction springs can also be included. These reactions spring may represent structural elements that resist movement of the pile. They are not intended to represent the soil.

Non-linear FEA in the cloud: The program solves for the pile response using non-linear finite element analysis. The calculations are performed on a cloud server. The the programs run efficiently on all devices connected to the internet.

Saving and sharing input data: Input data is saved as a project, with a *Project Name* and a *Run ID*. Projects are stored on a database server and users can access their projects across all of their devices. Projects can also be shared among users.

Auto-documentation: All input and output data can also be atomically downloaded in an Excel file (provided the device you are working on has Microsoft Excel installed). This allows for very rapid and thorough offline documentation.

Access: The program can be accessed by following links from www.geocalcs.com/lap. Users register their details. The program does not require the installation of any software other than a common web browser.

TERMS OF USE

LAP was developed by Dr James P. Doherty at the University of Western Australia. The program is made freely available for use as a research and teaching tool. For commercial applications, users must seek permission directly by contacting james.dohery@uwa.edu.au .

Although testing and validation of the *LAP* has been undertaken, it cannot be guaranteed that the program is free of errors. The developer offers no warrantee in relation to the use of *LAP* whatsoever and the developer cannot be held liable for errors that are based on the use of *LAP*.

GETTING STARTED

Outline

This section of the manual uses an example to provide some basic guidance for setting up and analysing a job in *LAP*. The example is illustrated in Figure 1 along with key input dimensions.

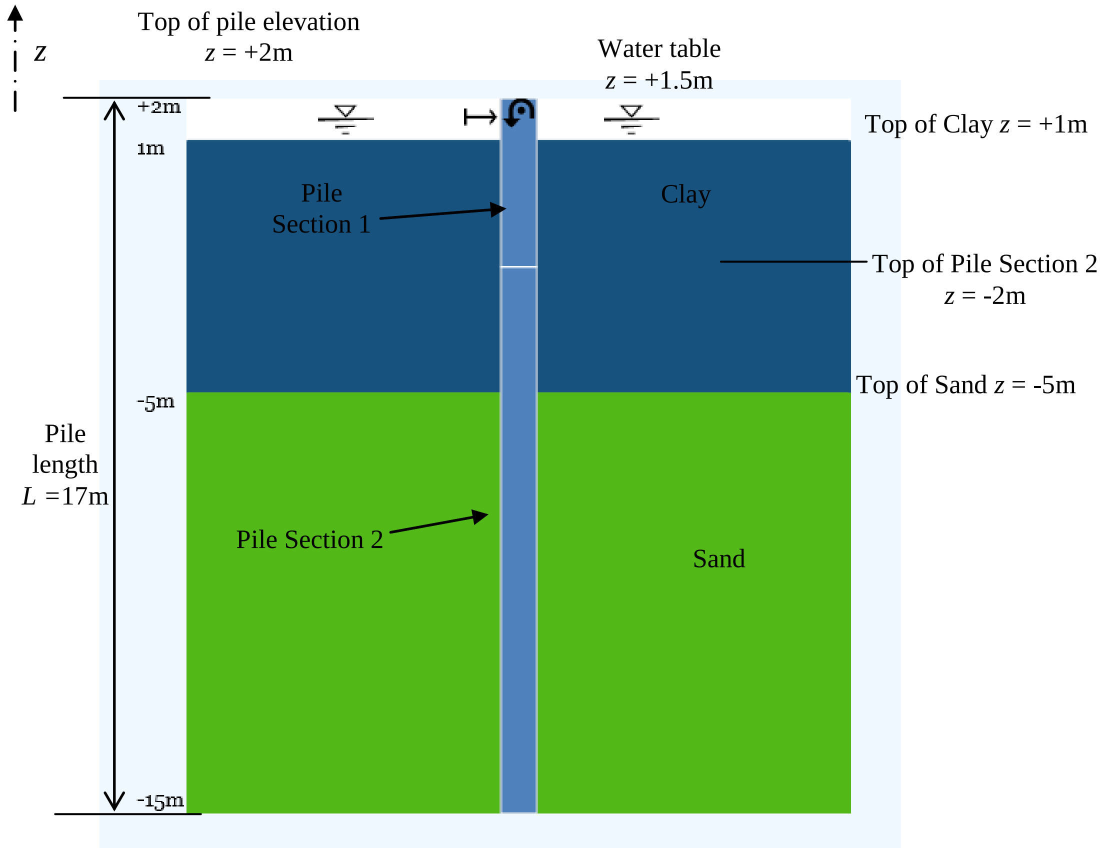

Figure 1: Example problem

Project

Immediately after in the "PROJECT" menu item will be active (Figure 2) and two options will be available. That is, we either load an old project (or manage old jobs including sharing them with other users) by selecting the "Load/share project" button or we "Create a new project".

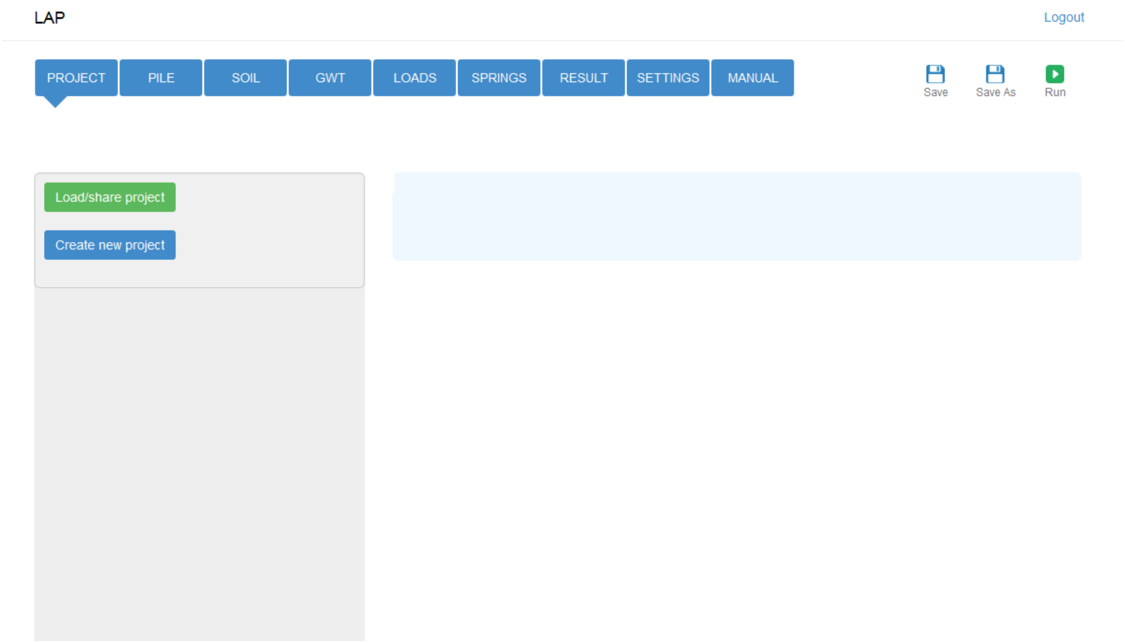

Figure 2: the PROJECT tab active

In this example, we start by creating a new project, which then prompts us to enter the “Project name” and “Run ID”. Values are entered as shown in Figure 3. After hitting Create, we are moved to the “PILE” menu item where the pile geometry and material propoerties are specified.

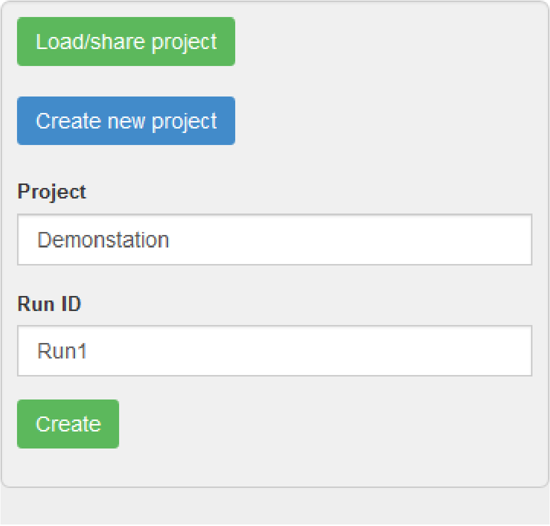

Project: Demonstation

Run ID: Run1

Figure 3: Project definition

Pile

The elevation of the top of the pile and the total length of the pile must first be defined (Figure 4). This positions the pile in space and later allows the soil, the water table and loads etc. to be positioned accordingly. In this example (see Figure 1) we set the elevation of the top of the pile to 2 m and the total length to 17 m. We must then define one or more section pile properties.

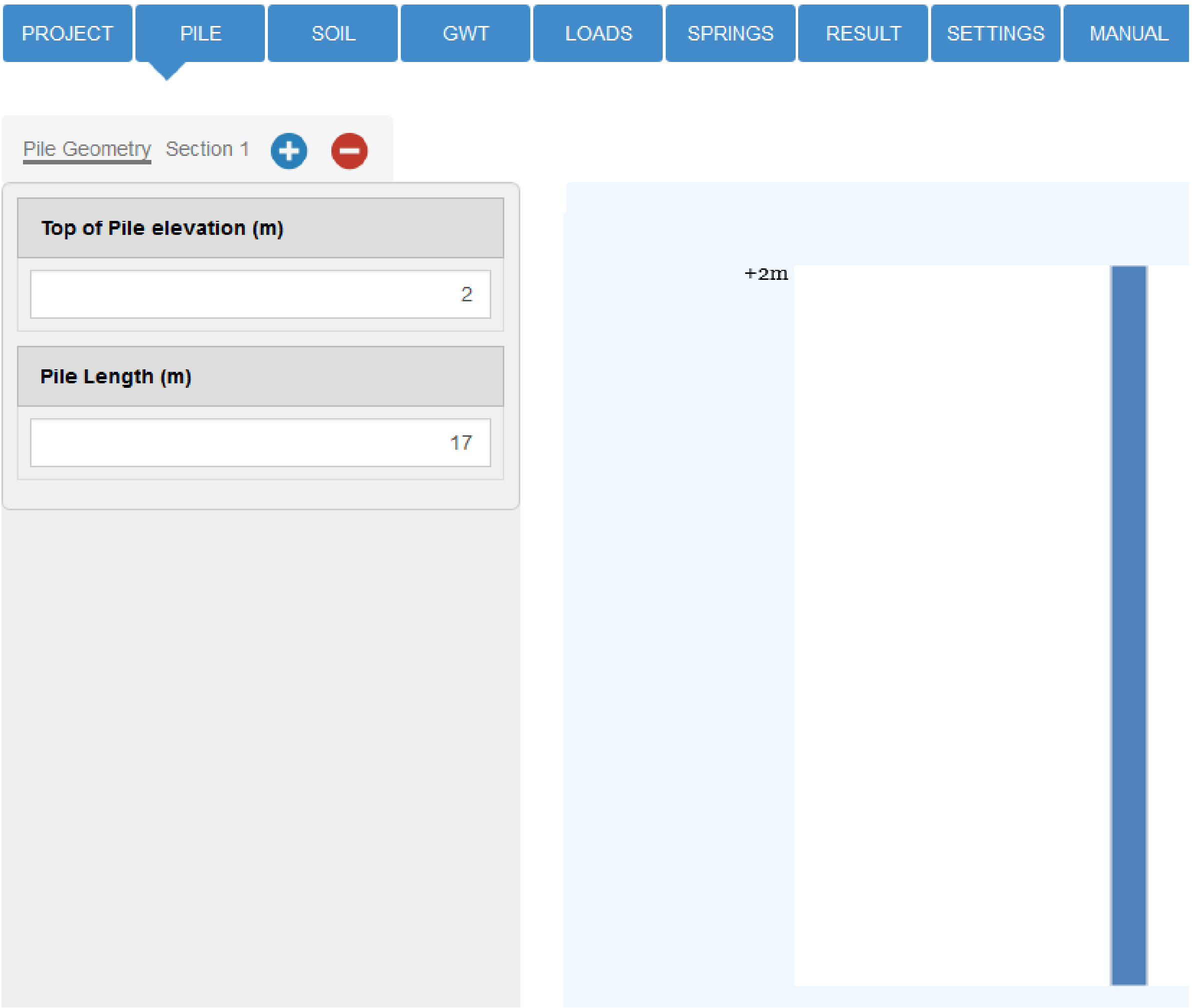

Top of Pile elevation (m): 2

Pile Length (m): 17

Figure 4: Pile position and total length

To define the first section, select “Section 1” (next to “Pile Geometry”). By default, the “Top of pile section (elevation (m))” for “Section 1” is equal to the top elevation of the pile (entered previously) and this cannot be edited. The length of the section is automatically shown. Users enter the diameter for the section and Type of section (i.e. elastic or elastic-perfectly plastic). In this example we choose a pile diameter of 1.3 m, select “Elastic” for type” and enter a flexural rigidly value (EI) of 50000 kNm^2 (see Figure 5).

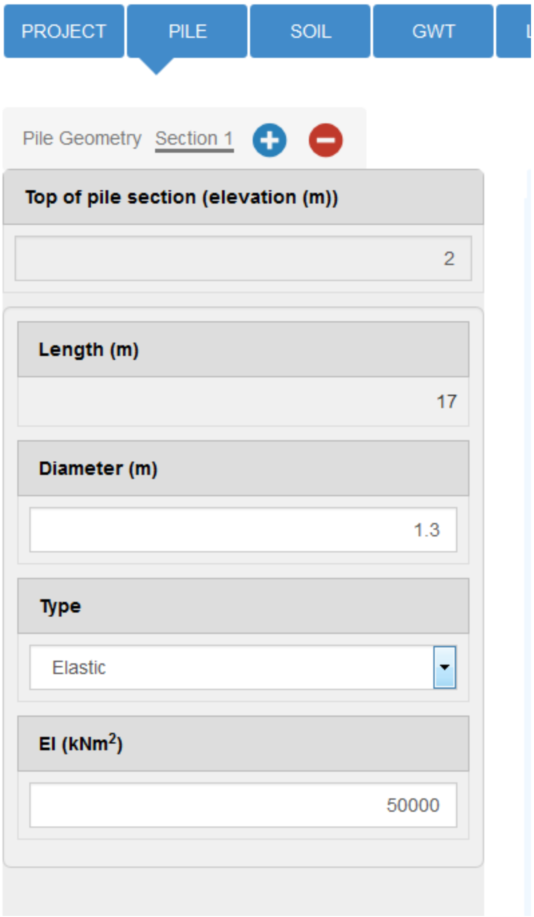

Top of pile section (elevation (m)): 2

Length (m): 17

Diameter (m): 1.3

Type: Elastic

EI (kNm^2): 50000

Figure 5: Section 1 Pile properties

To include another section in the model, select the “+” icon adjacent to “Section 1”. “Section 2” then appears in the submenu row and is automatically active. The “Top of pile section (elevation (m))” must be entered and this must be lower than the elevation of the top of the previous section (i.e. Section 1). In this example we select -2 m as the top of section elevation (Figure 6) so the length of Section 1 is 4 m. The length of the section is then displayed and a second “clickable” section appears in the canvas. Note; pile sections can be selected by clicking on the section in the canvas or by selecting from the menu bar.

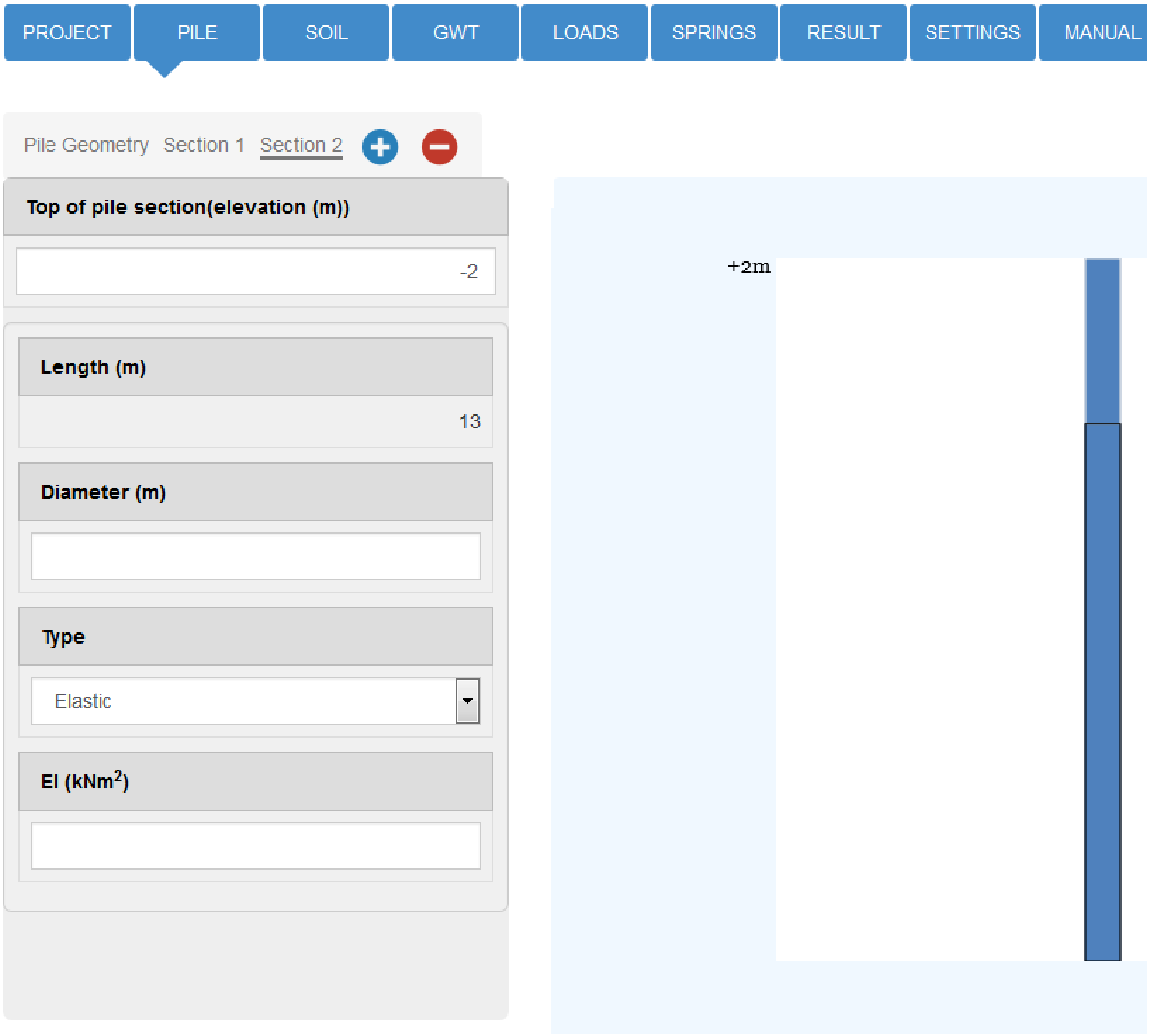

Top of pile section(elevation (m)): -2

Length (m): 13

Diameter (m):

Type: Elastic

EI (kNm^2):

Figure 6: Enter elevation of pile Section 2

The remaining input parameters for pile Section 2 are then entered, as shown in Figure 7. We then move to the “SOIL” menu to define the ground conditions.

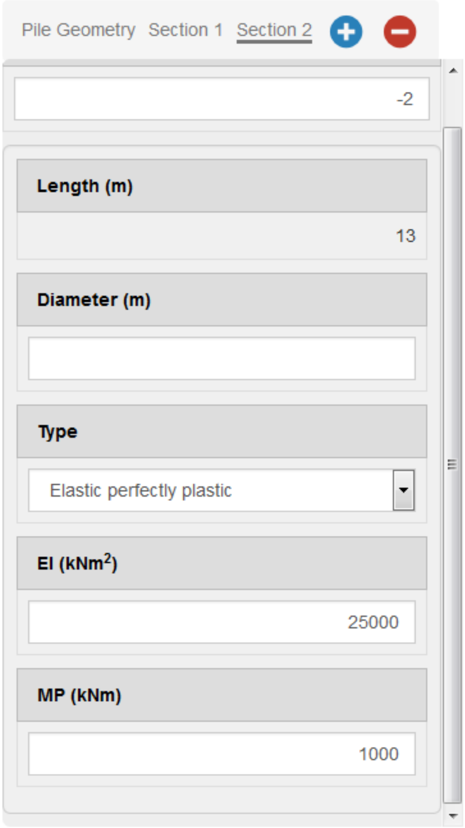

-2

Length (m)

13

Diameter (m)

Type

Elastic perfectly plastic

EI (kNm^2)

25000

MP (kNm)

1000

Figure 7: Parameters for Pile section 2

Soil

To begin with, the ground surface elevation is entered (see Figure 8). This positions the soil with respect to the (already defined) pile. In this example, we enter +1m as the Ground Surface Elevation. The canvas then shows the Pile with a top elevation of 2m and a total length of 17m embedded in soil with a ground surface of 1m.

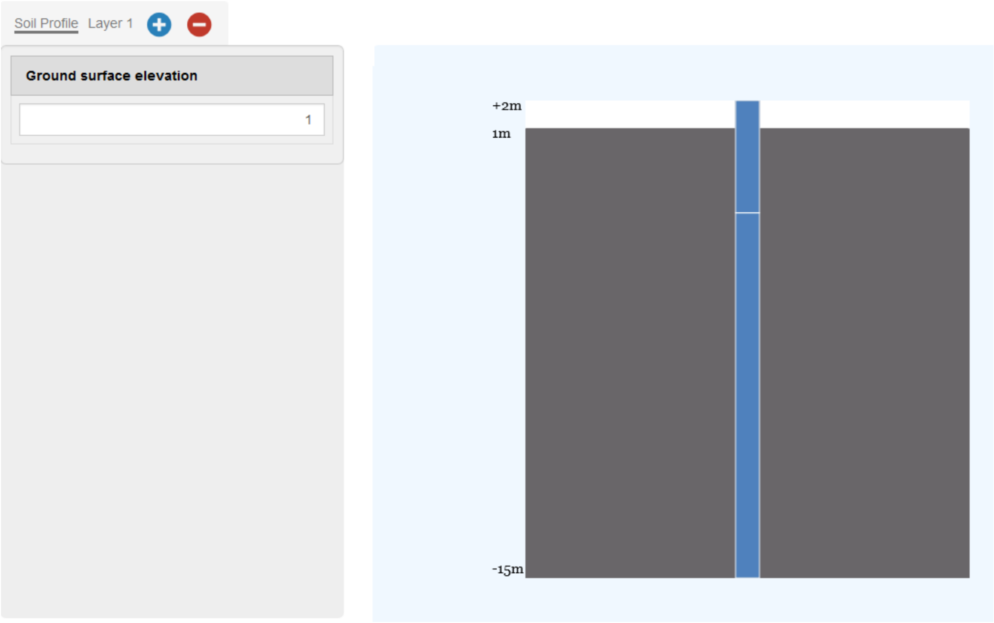

Ground surface elevation

1

Figure 8: defining the ground surface elevation

By default, there is one soil layer active in the model "Layer 1" (there must be at least one layer and maximum of 10 layers).

To define the first soil layer, select "Layer 1". The "Top of soil layer" is always fixed to be equal to the elevation of the ground surface for "Layer 1". This value cannot be edited. To define the soil properties of Layer 1, we specify the total unit weight of 16 kN/m^3 for this example. As Layer 1 is a "Soft Clay", we select "Clay" under the "Type" pull down menu, and then select "Soft" under the "Consistency" menu. This automatically populates the E50 and J parameters. In this example the undrained shear strength for the soft clay is 10 kPa at the ground surface and increases by 5 kPa/m with depth. These values are entered as shown in Figure 9.

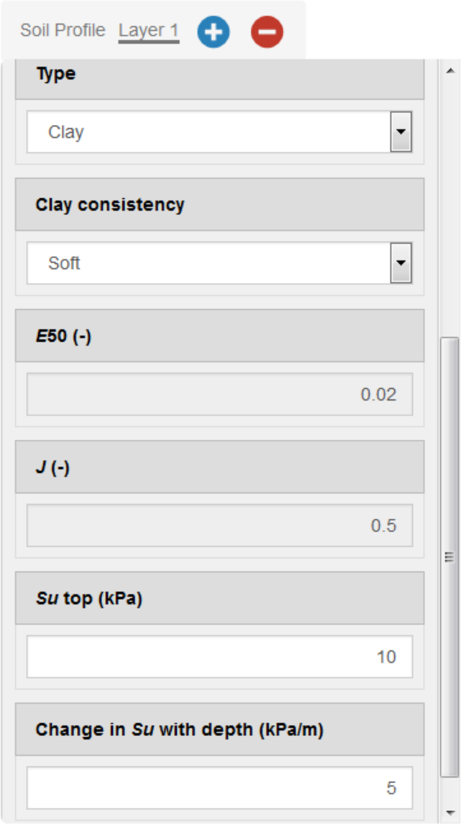

Type

Clay

Clay consistency

Soft

*E*50 (-)

0.02

J (-)

0.5

Su top (kPa)

10

Change in *Su* with depth (kPa/m)

5

Figure 9: Soil parameters for “Layer 1”

To add another soil layer we hit the “+” button, next to “Layer 1”. A value for the “Top of Layer” can then be entered. We enter -5 m (so the clay layer is 6m thick). Based on the example described above, we enter a total unit weight of 18 kN/m^3 and select “Sand API” as the soil Type, we then specify a friction angle of 35 degrees, as shown in Figure 10.

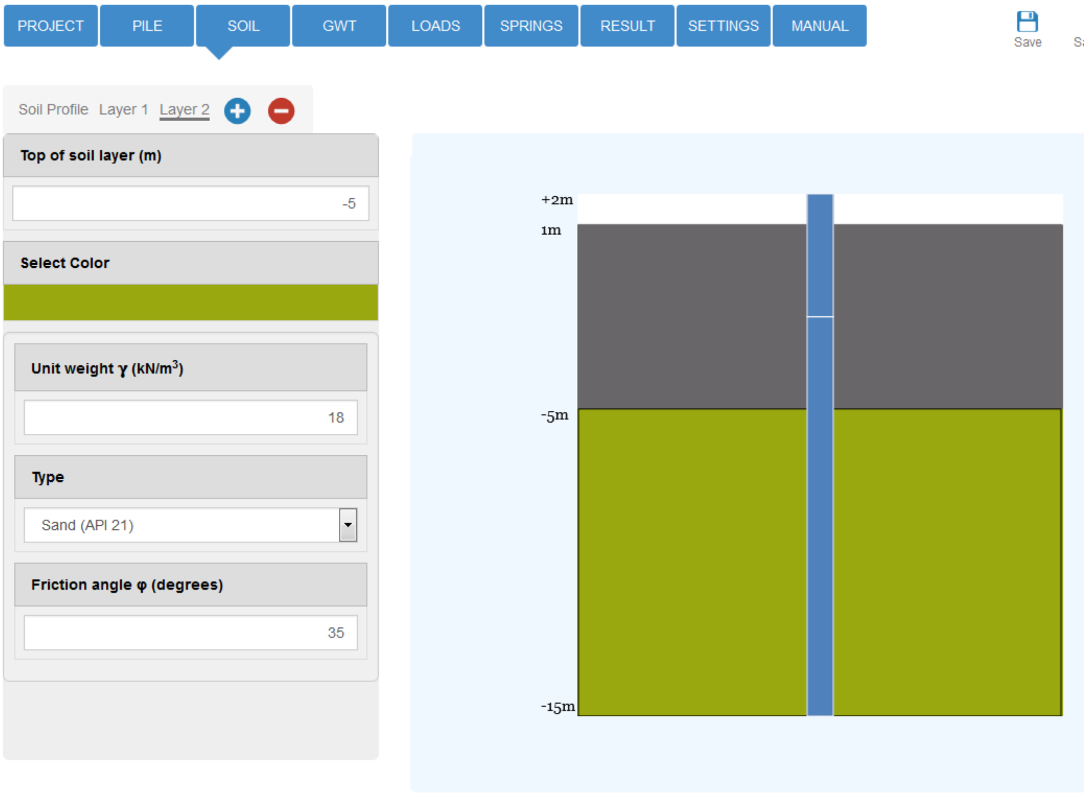

Top of soil layer (m): -5

Select Color

Unit weight γ (kN/m^3): 18

Type: Sand (API 21)

Friction angle φ (degrees): 35

Figure 10: Soil parameters for “Layer 2”

GWT

The elevation of the ground water table is specified under GWT, as shown in Figure 11.

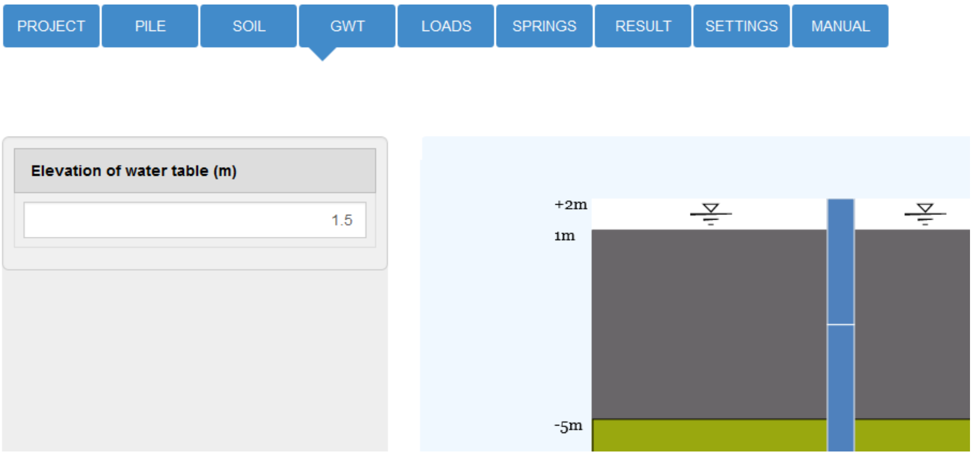

Elevation of water table (m): 1.5

Figure 11 specifying the elevation of the ground water table

Loads

We then select “LOADS” to define the loading conditions on the pile. Loads can be either applied force or moment, or prescribed displacement or rotation. In this example, no surcharge next to the pile is required, so this field is left blank (Figure 12).

Figure 12: Specifying a “Surcharge” load

The horizontal capacity of the fixed head pile is required, so a fairly arbitrary displacement of 1m is prescribed at the top of the pile (elevation of +2 m) (Figure 13). To specify fixed head condition, a rotation of zero is specified at +2 m (Figure 14). This completes the definition of the loads.

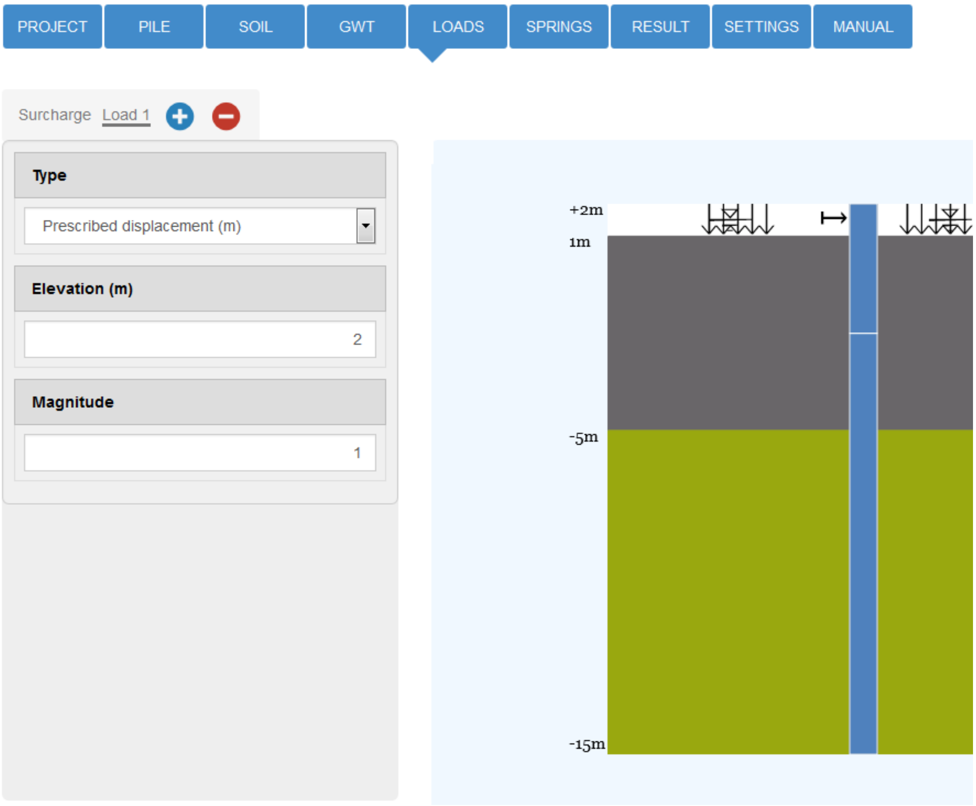

Type: Prescribed displacement (m)

Elevation (m): 2

Magnitude: 1

Figure 13: Specifying a prescribed displacement

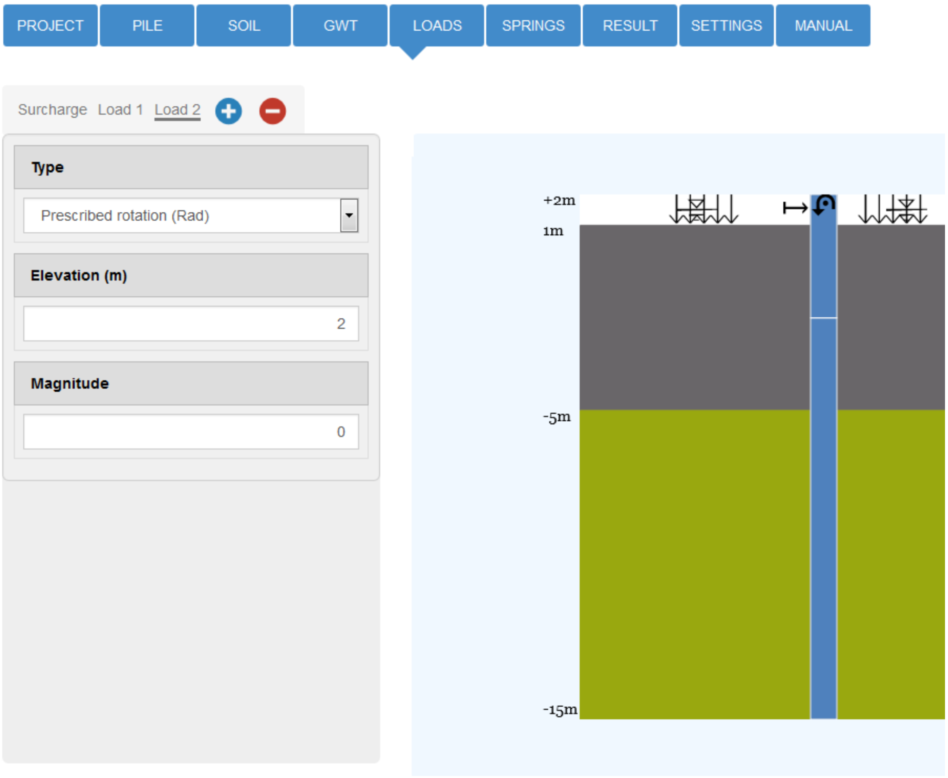

Type: Prescribed rotation (Rad)

Elevation (m): 2

Magnitude: 0

Figure 14: Specifying a prescribed rotation

Springs

SPRINGS can be used to define linear elastic reactions springs. They are not needed for representing the soil. They can, for example, be used to represent a tie or an anchor attached to the pile at any depth. In this example, springs are not needed, so this option is left blank (see Figure 15).

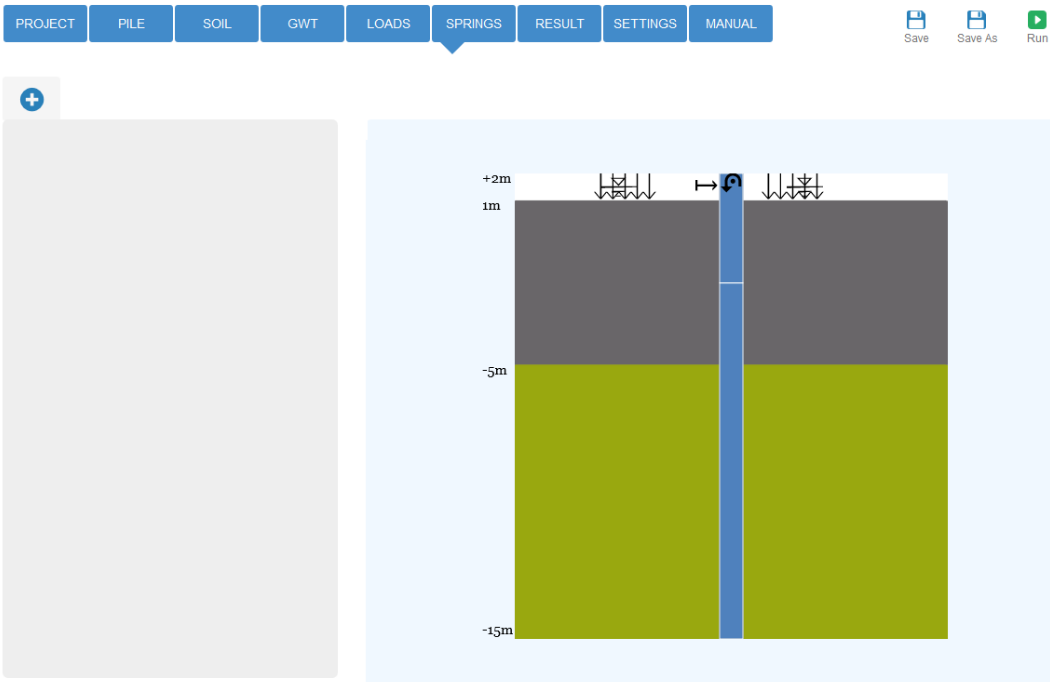

Figure 15: Reaction “springs”

Settings

Select “SETTINGS” to review the solution settings options, as shown in Figure 16. The “Theoretical” section of this manual describes in detail the numerical procedure used by LAP, where the precise definition of the SETTINGS parameters are given.

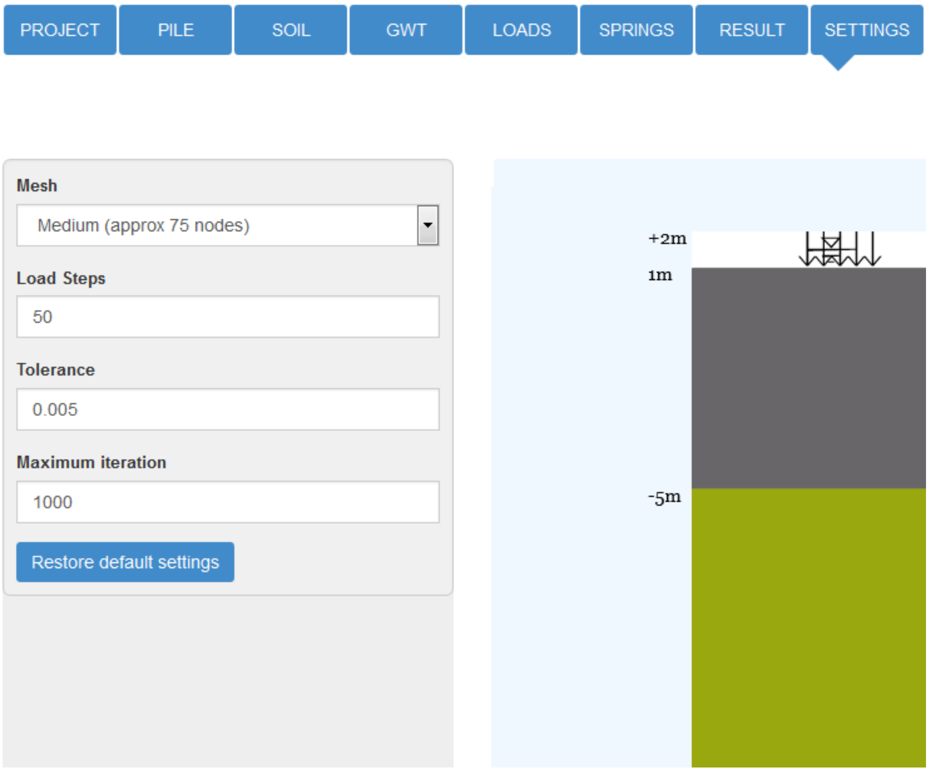

Mesh
Medium (approx 75 nodes)

Load Steps
50

Tolerance
0.005

Maximum iteration
1000

Figure 16: Default solution settings

Results

The analysis is executed by selecting the “Run” button in the upper right corner. (Prior to executing the analysis, the RESULTS menu cannot be accessed). After selecting Run, a “loading” icon is shown to indicate the analysis is being conducted. Once compete, the RESULTS menu become active. If the analysis completed successfully, a green tick will appear on in the left side (see Figure 17). Users can select one of five summary plots to rapidly review the results of the analysis. Figure 17 shows the load-displacement response of the pile, where the load is computed from the soil reaction pressures and the displacement is the maximum displacement along any section of the pile (usually, but not always, the top of the pile).

Analysis complete successfully

Figure 17: Screen shot with RESULTS selected

Detailed results can be "Exported to Excel". The excel sheet contains three tabs. The first tab ("Geometry") documents the Project name and run ID, the solution settings, the basic geometry associated with the pile, soil and loads.

The second sheet is the "Summary results" sheet. This tabulates the time step which ranges between 0 and 1, where 0 is no load applied and 1 is full load applied. The number of iterations for each load step is shown, along with the maximum pile displacement and the total horizontal force. The pile properties, along with the bending moment, shear force and pile displacement at each time step are presented in the "pileOutput" sheet. The input parameters and the response of each soil p-y curve is presented in detail in the "soilSpringOutput" sheet.

MODELLING

Defining geometry

The pile geometry is defined by specifying the elevation of the top of the pile (z_p^t), along with the pile length (L). This defines the position and size of the pile, around which soil, loads etc. can be later defined. The pile can have up to ten sections, each with a different diameters and material properties (flexural stiffness EI and plastic moment capacity M_p). The pile sections are numbered in sequence from the top of the pile to the bottom. Figure 18 shows an example of a pile with three sections. The geometry of each section is specified by entering the elevation of the top of each section z_p^i, where i correspond to the section number. The top of Section 1 is always equal to the top of the pile ($z_p^1 = z_p^t$). The length of each section is automatically calculated.

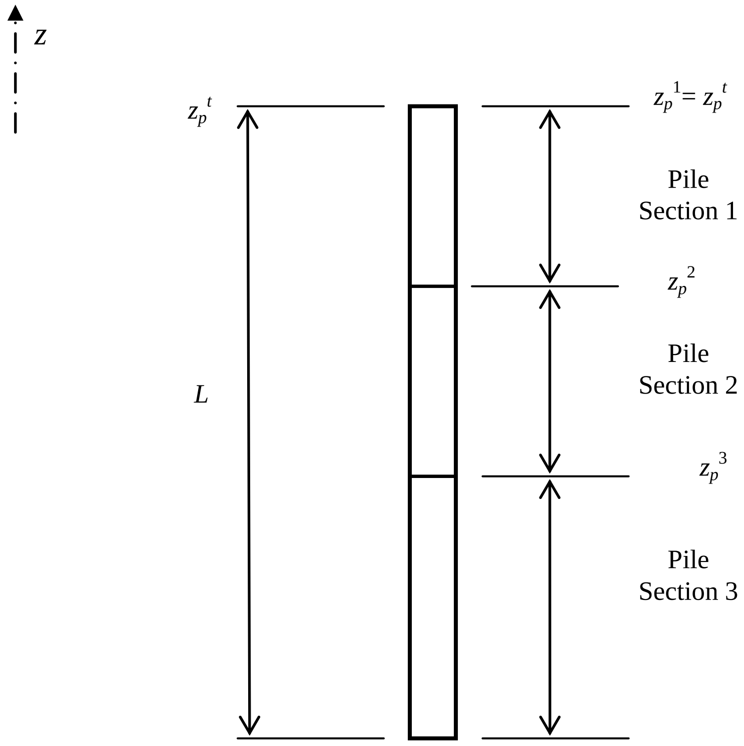

Figure 18: Pile geometry definition

Soil geometry is defined in a similar way. That is, the elevation of the ground surface is specified along with the elevation of the top of each soil layer. Soil layers are number in sequence from top to bottom. The elevation of the ground surface (also the top of "Layer 1") must be located between z_p^t (top of the pile) and z_p^t - L (bottom of the pile). This is to ensure that some of the pile is embedded in the ground. The ground surface cannot be above the top of the pile. However surcharge loads can be applied to approximate the total stress of the ground above a pile if this is needed.

Soil profile and initial stress

The geometry of the model is defined in terms of elevation coordinate *z*, which is positive in the upward direction. However, it is more convenient and intuitive to define soil properties and pore pressures in terms of depth below the ground surface (*d*), measured positively in the downward direction, as shown in Figure 19. The depth below the ground water table is defined as d_w. The pore pressure in the *LAP* is zero above the water table and increases hydrostatically below the water table. i.e.

$$u = \gamma_w d_w \quad (1)$$

for $d_w > 0$, where γ_w is the unit weight of water (taken as 10 kN/m^3). The soil *p-y* curves usually depend on the depth below ground surface (*d*) and the effective stress effective vertical stress (σ'_v) at that depth. It is therefore important to be clear on how the vertical effective stress is calculated at any particular depth in LAP. The vertical effective stress (σ'_v) at any depth *d* is given by

$$\sigma'_v = \sigma'^s_v + \int_0^d \gamma(d)\, \mathrm{d}d - u(d) + u^s \quad (2)$$

Where

- σ'^s_v is the “surcharge” specified under the “LOADS” menu.
- $u(d)$ is the pore pressure at depth d
- u^s is the pore pressure at the ground surface, which will be zero if the water table is below the ground surface or non-zero if the water table is above the ground surface
- $\gamma(d)$ is the total unit weight of a soil layer.

Equation (2) ensures that the vertical effective stress at the ground surface is always equal to the surcharge (σ'^s_v) specified under the “LOADS” menu. If this value is left blank, the vertical effective stress at the ground surface is zero regardless of whether the water table is above or below the ground surface. This is because at the ground surface $u^s = u(d{=}0)$ and the terms cancel in Equation (2). The effective vertical stress is clearly influenced by the position of the water table. However, if the water table is above the ground surface, the distance above the ground surface does not influence the effective stress.

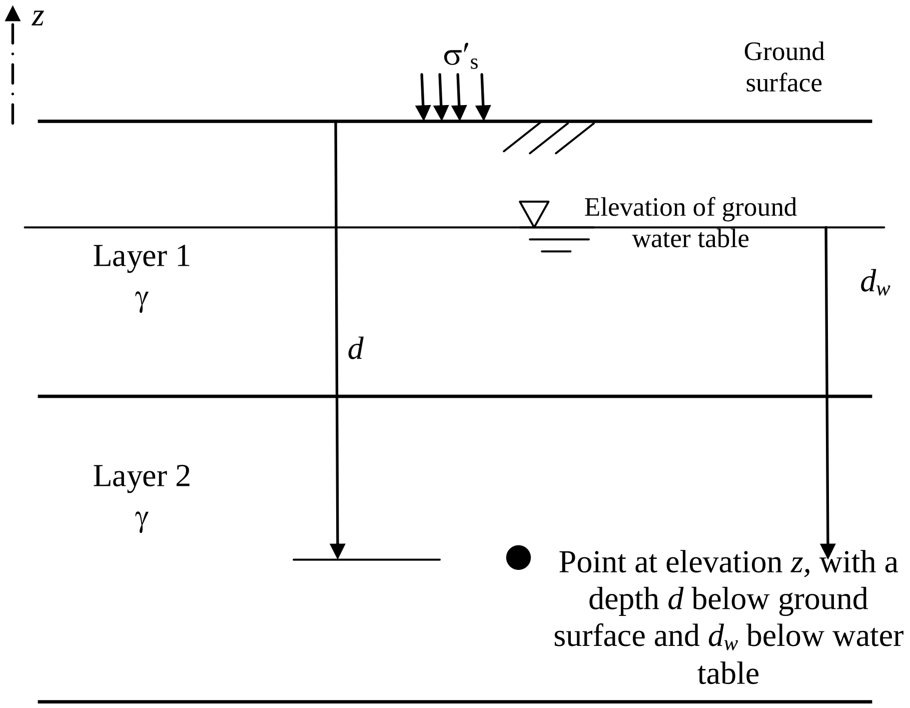

Figure 19: Soil stress and pore pressure definition

The vertical effective stress used in the model can be inspected the in downloaded Excel, in the “soilSpringOutput” tab after the analysis has been completed, as shown in Figure 20.

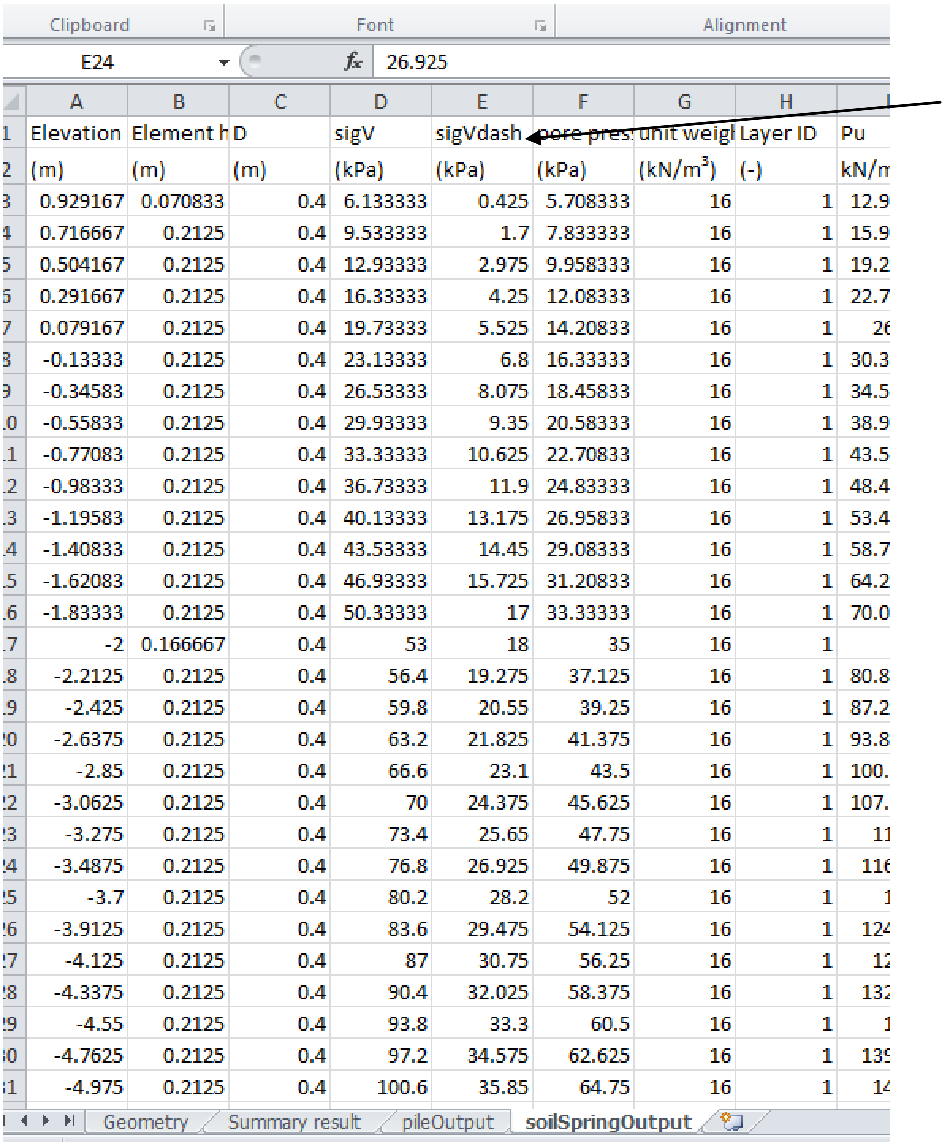

sigVdash= σ'_v

	A	B	C	D	E	F	G	H	I
1	Elevation	Element h	D	sigV	sigVdash	pore pres	unit weig	Layer ID	Pu
2	(m)	(m)	(m)	(kPa)	(kPa)	(kPa)	(kN/m^3)	(-)	kN/m
3	0.929167	0.070833	0.4	6.133333	0.425	5.708333	16	1	12.9
4	0.716667	0.2125	0.4	9.533333	1.7	7.833333	16	1	15.9
5	0.504167	0.2125	0.4	12.93333	2.975	9.958333	16	1	19.2
5	0.291667	0.2125	0.4	16.33333	4.25	12.08333	16	1	22.7
7	0.079167	0.2125	0.4	19.73333	5.525	14.20833	16	1	26
3	-0.13333	0.2125	0.4	23.13333	6.8	16.33333	16	1	30.3
9	-0.34583	0.2125	0.4	26.53333	8.075	18.45833	16	1	34.5
.0	-0.55833	0.2125	0.4	29.93333	9.35	20.58333	16	1	38.9
.1	-0.77083	0.2125	0.4	33.33333	10.625	22.70833	16	1	43.5
.2	-0.98333	0.2125	0.4	36.73333	11.9	24.83333	16	1	48.4
.3	-1.19583	0.2125	0.4	40.13333	13.175	26.95833	16	1	53.4
.4	-1.40833	0.2125	0.4	43.53333	14.45	29.08333	16	1	58.7
.5	-1.62083	0.2125	0.4	46.93333	15.725	31.20833	16	1	64.2
.6	-1.83333	0.2125	0.4	50.33333	17	33.33333	16	1	70.0
.7	-2	0.166667	0.4	53	18	35	16	1	
.8	-2.2125	0.2125	0.4	56.4	19.275	37.125	16	1	80.8
.9	-2.425	0.2125	0.4	59.8	20.55	39.25	16	1	87.2
0	-2.6375	0.2125	0.4	63.2	21.825	41.375	16	1	93.8
1	-2.85	0.2125	0.4	66.6	23.1	43.5	16	1	100.
2	-3.0625	0.2125	0.4	70	24.375	45.625	16	1	107.
3	-3.275	0.2125	0.4	73.4	25.65	47.75	16	1	11
4	-3.4875	0.2125	0.4	76.8	26.925	49.875	16	1	116
5	-3.7	0.2125	0.4	80.2	28.2	52	16	1	1
6	-3.9125	0.2125	0.4	83.6	29.475	54.125	16	1	124
7	-4.125	0.2125	0.4	87	30.75	56.25	16	1	12
8	-4.3375	0.2125	0.4	90.4	32.025	58.375	16	1	132
9	-4.55	0.2125	0.4	93.8	33.3	60.5	16	1	1
0	-4.7625	0.2125	0.4	97.2	34.575	62.625	16	1	139
1	-4.975	0.2125	0.4	100.6	35.85	64.75	16	1	14

Figure 20: Screen shot of an Excel file generated by *LAP*

Units

The basic units in LAP are length and force. The units adopted are

- Length in metres (m)
- Force in kilo Newtons (kN)

Sign Convention

Horizontal forces and displacements are positive when they act from left to right as shown in Figure 21. Applied moments and rotations are positive in the clockwise direction (see Figure 21).

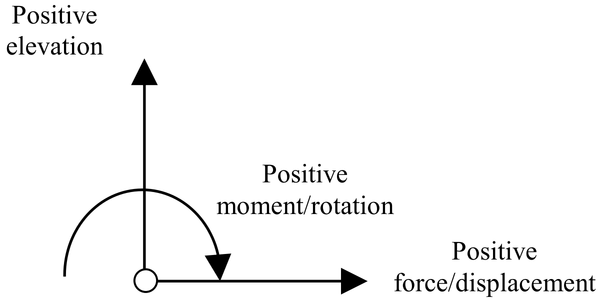

Figure 21: External sign convention

This means, for example, that a 100 kN force in the positive direction acting 50 m above the ground surface could be replaced with the same horizontal force (100 kN) and a positive moment of 5000 kNm at the ground surface, as illustrated in Figure 22.

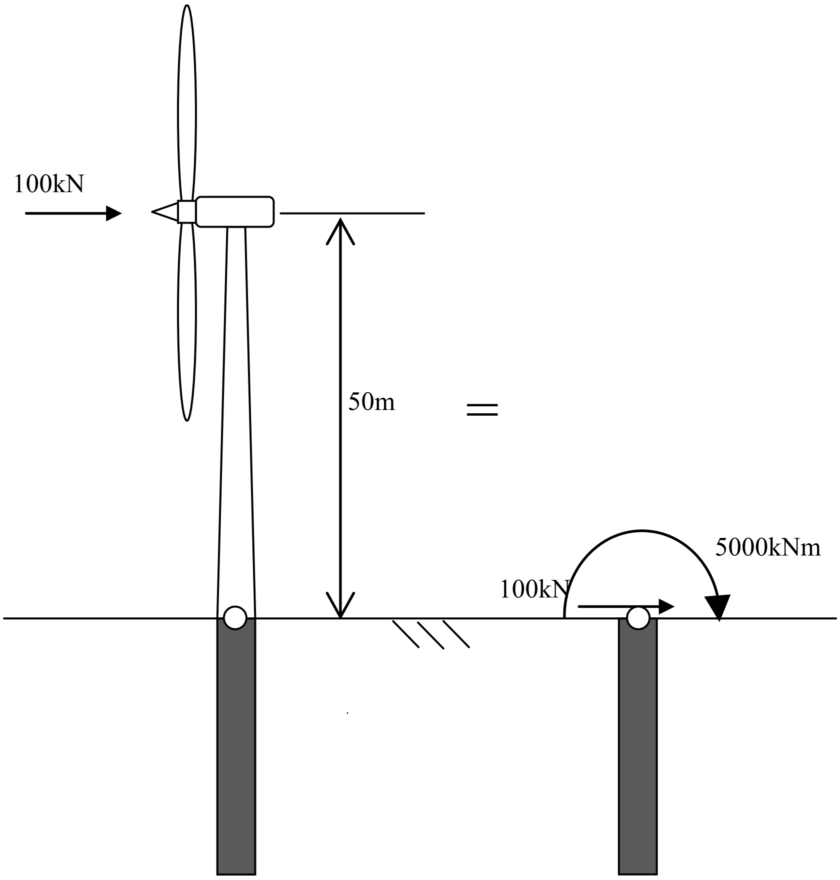

Figure 22: Example of LAP force and moment sign convention

The "internal" sign convention for bending moment and shear forces is shown in Figure 23.

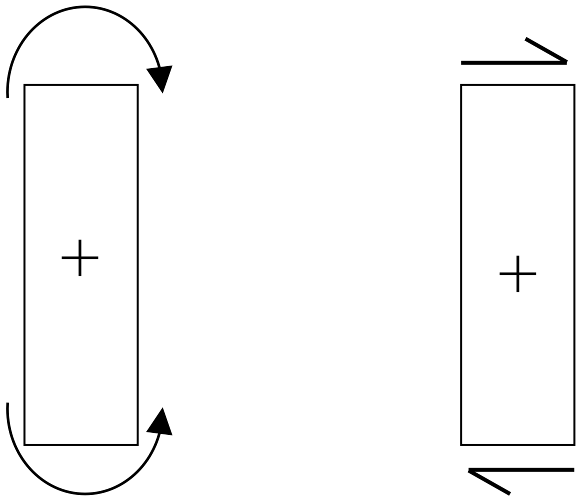

Positive bending moment convention

Positive shear force convention

Figure 23: Positive internal convention

PILE PROPERTIES

The pile is model as a series of beam elements. The moment-curvature response of an elastic perfectly-plastic beam is shown in Figure 24. This response is defined by the flexural stiffness EI, which represents the slope of the elastic portion of the curve, and the maximum moment that can be sustained, M_p. If the pile is assumed to be elastic, then M_p is not needed.

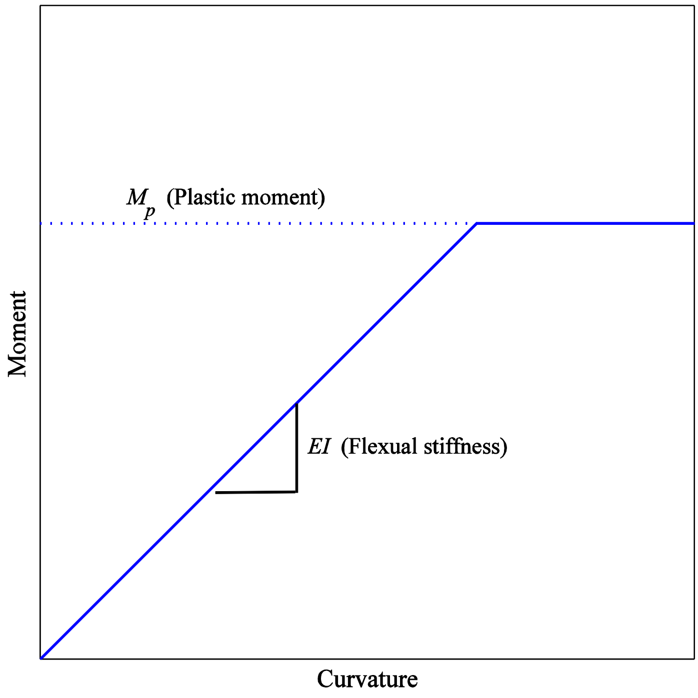

Figure 24: Elastic perfectly plastic moment-curvature response

SOIL SPRINGS

Outline

LAP includes a number of soil *p-y* curves (load transfer functions) that are commonly used in practice. A number of more recently developed *p-y* curves are also included that can be specified by directly pasting in Cone Penetration Test (CPT) data. Users also have the option to specify their own *p-y* curves. This section described each *p-y* load transfer function implemented in *LAP*.

Elastic perfectly-plastic (calculated)

The Elastic perfectly-plastic (calculated) *p-y* curves give a bi-linear load-displacement response as shown in Figure 25. This bi-linear response is defined by an ultimate load p_u and the slope K (stiffness) of the initial elastic portion of the curve. The spring input parameters are described in Table 1.

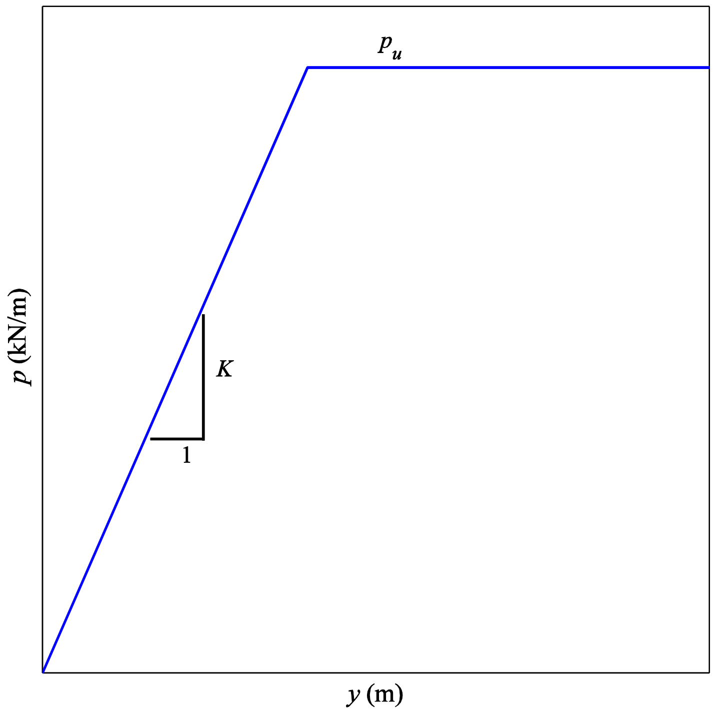

Figure 25: *p-y* response for Elastic perfectly plastic spring model

The ultimate lateral resistance p_u (per unit pile length) is calculated as

$$p_u = (K_q \sigma_v'(z) + cK_c)D \quad (3)$$

where $\sigma_v'(z)$ is the vertical effective stress, c is the soil cohesion and D is the pile diameter. The passive resistance coefficients for the frictional (K_q) and cohesive (K_c) soil strength components are a function of the depth below ground surface (d), the pile diameter (D) and friction angle (ϕ). In *LAP*, values for K_q and K_c are based on values established by (Brinch Hansen, 1961), and are plotted in Figure 26 and Figure 27, respectively. The stiffness of the elastic portion of the curve is defined by input parameter K. A complete list of parameters is given in Table 1.

Table 1: Input parameters for Elastic perfectly-plastic (calculated)

Parameter (units)	Description
K (kN/m)	Stiffness
ϕ (degrees)	Friction angle
c_t (kPa)	Cohesion at top of layer
d_c (kPa/m)	Change in cohesion with depth

The cohesion in Equation (3) can vary through the depth of the soil layer. This is defined by specifying the value of cohesion at the top of the soil layer (c_t) and the rate of increase in cohesion with depth (d_c). This is illustrated in Figure 28.

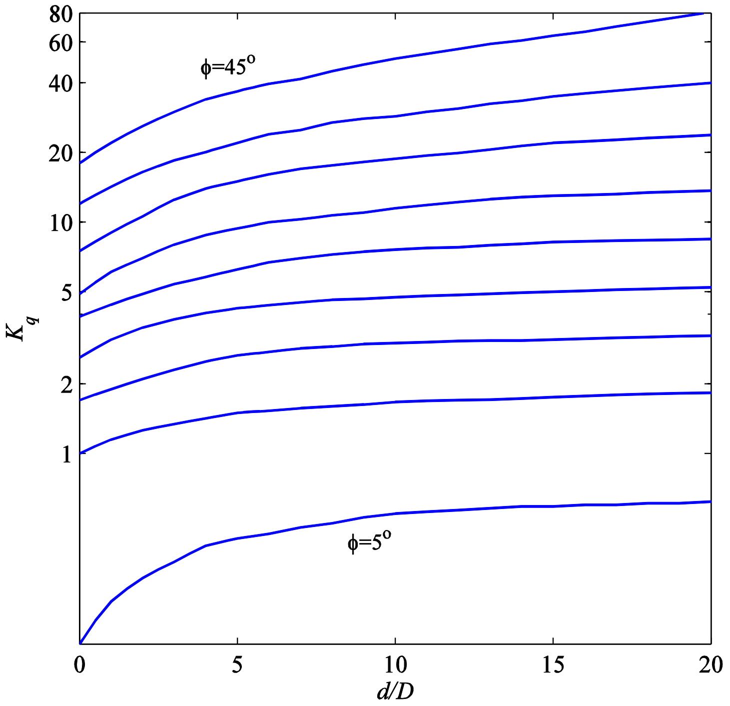

Figure 26: Brinch Hansen K_q values.

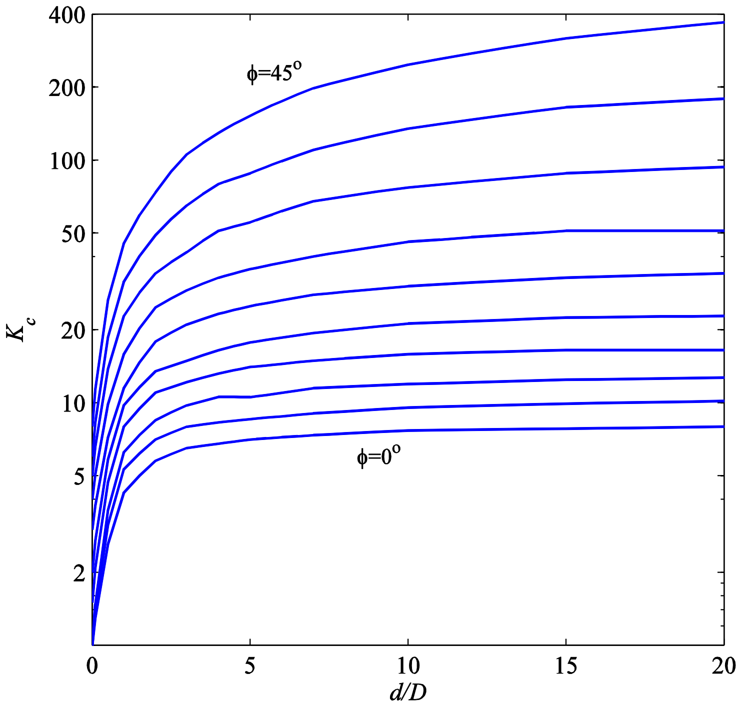

Figure 27: Brinch Hansen K_c values.

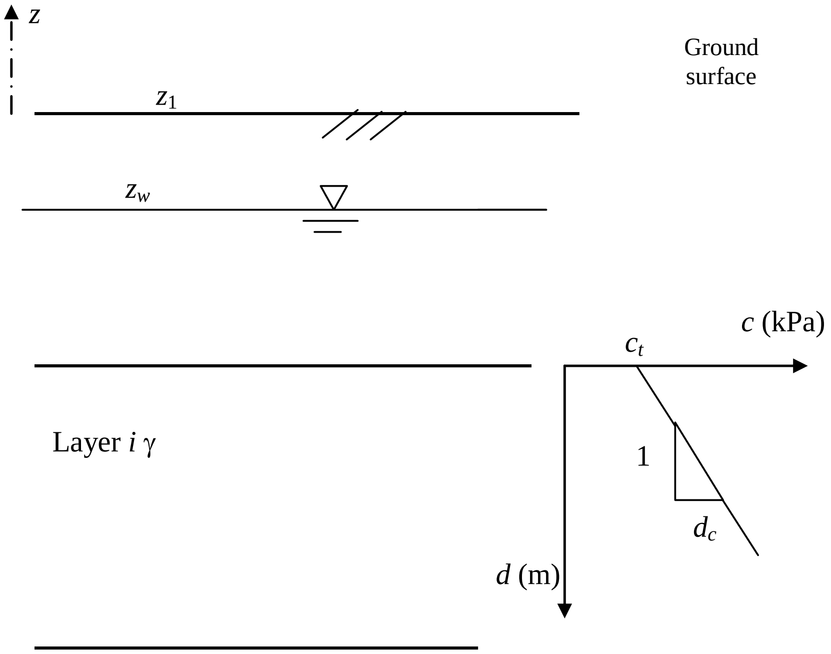

Figure 28: variation of cohesion with in a soil layer

Elastic perfectly-plastic (user defined)

The *p*-*y* curves for “Elastic perfectly plastic (user defined)” springs are of an identical form to the Elastic perfectly plastic (calculated), as illustrated in Figure 25. However, the values of the K_q and K_c are direct inputs, rather than being calculated using the (Brinch Hansen, 1961) values. The input parameters are listed in Table 2. Note, because friction angle is not needed to define the K_q and K_c values, it is not included as a material input parameter.

Table 2: Input parameters for “Elastic perfectly-plastic (user defined)”

Parameter (Units)	Description
K (kN/m^2)	Stiffness
K_q (-)	Frictional resistance coefficient
K_c (-)	Cohesive resistance coefficient
c (kPa)	Cohesion at top of soil layer
d_c (kPa/m)	Change in cohesion with depth

Sand API 21

The Sand (API 21) *p-y* curves are based on recommendation published in the, (API, 2011), which were originally based on the work of (Reese et al., 1974) and (O'Neill and Murchison, 1983). API (2011) notes that the data on which these *p-y* curves were developed consisted of tests on the lateral response of free-head piles in clean sands, with friction angles ranging from 34^o to 42^o degree, as determined by shear box tests, drained triaxial tests or correlations with in-situ tests. Extrapolation of these data to soils outside the limit of experience, particularly to sands with angles of friction less than 30^o, should be done with caution. The API code also notes that the spring capacity may be unconservative for layered soils, when the sand is overlain by soft clay.

For "Sand API 21", the ultimate lateral capacity (p_u) is defined as

$$p_u = \min\begin{cases}(C_1 d + C_2 D)\ \sigma_v' \\ C_3 D\ \sigma_v'\end{cases} \quad \text{......(4)}$$

where C_1, C_2 and C_3 are coefficients given by

$$C_1 = \frac{\tan^2\beta\tan\alpha}{\tan(\beta-\phi)} + K0\left(\frac{\tan\phi\tan\beta}{\cos\alpha\tan(\beta-\phi)} + \tan\beta(\tan\phi\sin\beta - \tan\alpha)\right) \quad \text{......(5)}$$

$$C_2 = \frac{\tan\beta}{\tan(\beta-\phi)} + K_a \quad \text{......(6)}$$

$$C_3 = K_a\left(\tan^8\beta - 1\right) + K0\tan\phi\tan^4\beta \quad \text{......(7)}$$

where $K0 = 0.4$ and, $\alpha = \phi/2$, $\beta = 45 + \phi/2$ and $K_a = (1 - \sin\phi)/(1 + \sin\phi)$. Figure 29 plots the values of these coefficients over a range of friction angles.

The p-y curve is defined as

$$p = p_u A \tanh\left(\frac{kdy}{Ap_u}\right) \quad \text{......(8)}$$

where parameter k is the rate of increase of initial modulus of subgrade reaction with depth. (API, 2011) provides recommended values as a function of friction angle (see Table 3). In LAP, k is automatically calculated by interpolation using the specified friction angle and the data in Table 3.

For the "Static" option, the paramater A is defined as

$$A = \max\begin{cases}3 - 0.8d/D \\ 0.9\end{cases} \quad \text{......(9)}$$

For the “Cyclic” option, *A* = 0.9.

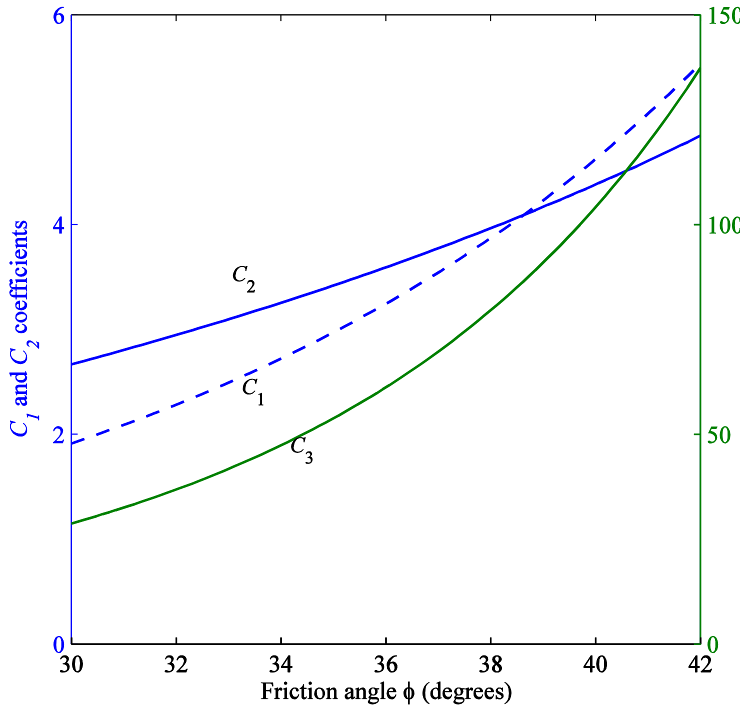

Figure 29: API Sand 21 coefficients

Table 3: Rate of increase of initial modulus of subgrade reaction with depth

Friction angle ϕ (degrees)	*k* (kN/m^3)
25	5400
30	11000
35	22000
40	45000

For the “Static” option, when $A > 1$ (i.e. for low *d/D* values) Equation (8) allows $p > p_u$. This creates some confusion, as p_u is defined as the ultimate lateral bearing pressure. LAP therefore includes two static options; one which allows $p > p_u$ and another which cuts *p* off at the lesser of Ap_u or p_u.

Static (p <= $A.p_u$)

The “Static A.pu” option uses Equation (8) without a cutoff. This allows $p > p_u$ for $A > 1$. The p-y curve is formed by generating ten evenly spaced values for y between 0 and y= $3.0Ap_u/kd$. An 11th value of y= $5Ap_u/kd$ is also included. The final normalised form of the p-y curve is shown in Figure 30.

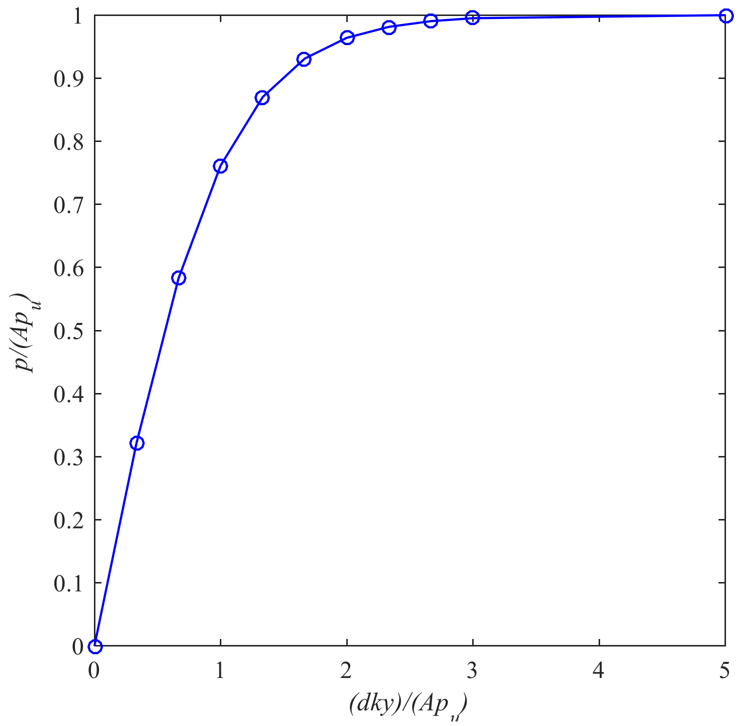

Figure 30: API static with no cut off at pu (i.e. p<=Apu)

Static cutoff (p <= min(pu,Apu))

The “Static cutoff at pu” option uses equation (8) for $p \leq p_u$. The curves are formed by first computing a value for y satisfying $kdy/p_u = 3/A$. A curve is then form between zero and this value for y in 9 equal increments. A final value for y satisfying $kdy/p_uA = 5$ is then found, completing the curves illustrated in Figure 31 for a range of A values.

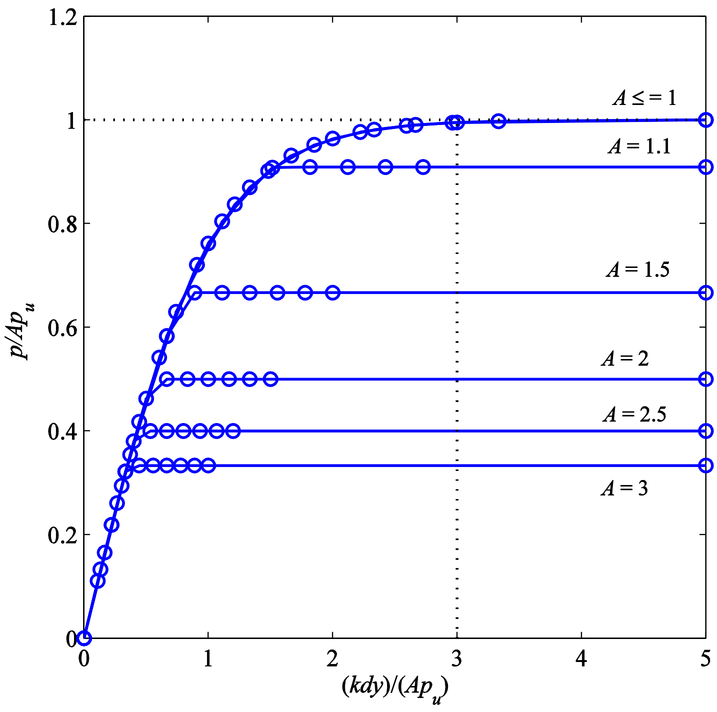

Figure 31: Nomralised form of API Sand 21 with p<= pu

API Sand has a single input parameter, ϕ, as listed in Table 4.

Table 4: Input parameters for Sand API21

Parameter (Units)	Description
ϕ (degrees)	Friction angle

Clay API

The *p*-*y* curves for Clay API are based on the equations established by (Matlock, 1970), where the ultimate resistance varies from $3S_uD$ to $9S_uD$ as the depth below ground surface (d) increases. That is

$$p_u = \min\begin{cases} 3S_uD + \sigma_v'D + JdS_u \\ 9S_uD \end{cases} \quad \text{......(10)}$$

where S_u is the undrained shear strength and D is the pile diameter. The value of S_u is defined at a particular depth by specifying the undrained shear strength at the top of the soil layer S_{ut} and a rate of increase of S_u with depth within the layer d_{Su}. This is similar to the specification of cohesion for the Elastic perfectly-plastic *p*-*y* curves (see Figure 28).

The *p*-*y* curves are generated from data in Table 5 for short terms static loading.

Table 5: API Clay *p-y* data for short-term static loading

p/p_u	y/y_c
0.00	0.0
0.23	0.1
0.33	0.3
0.50	1.0
0.72	3.0
1.00	8.0
1.00	∞

For cases where equilibrium has been reached under cyclic loads, the *p*-*y* curves are generated from data in Table 6.

Table 6: *p-y* data for equilibrium conditions of cyclic loading

$d \geq d_r$		$d < d_r$	
p/p_u	y/y_c	p/p_u	y/y_c
0.00	0.0	0.00	0.0
0.23	0.1	0.23	0.1
0.33	0.3	0.33	0.3
0.50	1.0	0.50	1.0
0.72	3.0	0.72	3.0
0.72	∞	$0.72\, d/d_r$	15.0
		$0.72\, d/d_r$	∞

The value of y_c is calculated as

$$y_c = 2.5\, E_{50}\, D \quad \text{......(11)}$$

E_{50} is an input parameter that defines the strain at 50% of the maximum stress. A complete list of input parameters is given in Table 7. The value of d_r in Table 6 is depth (d) below ground surface where

$$3S_uD + \sigma_v'D + JdS_u = 9S_uD \quad \text{..........} (12)$$

Table 7: Parameters for Clay API

Parameter (Units)	Description
*E*50 (-)	Strain at 50% maximum stress
J (-)	Empirical parameter
Su (kPa)	Undrained shear strength at top of soil layer
d_{su} (kPa/m)	Change in undrained shear strength with depth

The general form of *p-y* curve for both static and cyclic loading is shown in Figure 32.

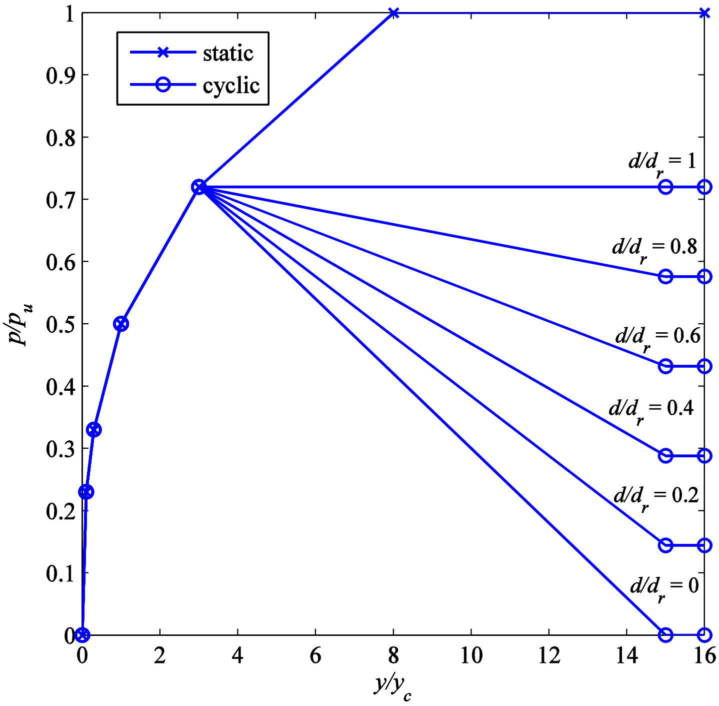

Figure 32: Form of *p-y* curve for Clay API

In *LAP*, the parameters *J* and E_{50} can be selected manually. Alternatively, users can specify the clay consistency (soft, firm, stiff or hard) with the resulting parameters listed in Table 8 used.

Table 8: Input parameters based on consistency

Consistency	J	E_{50}
Soft	0.5	0.02
Firm	0.5	0.01
Stiff	0.25	0.005
Hard	0.25	0.004

Soft Clay (Jeanjean)

(Jeanjean, 2009) developed *p-y* curves based on a series of model centrifuge tests and finite element simulations. The *p-y* curves are given by

$$p = p_u \tanh\left(\frac{G_{max}}{100Su}\left(\frac{y}{D}\right)^{0.5}\right) \text{.....................(13)}$$

where G_{max} is the small strain shear modulus, Su is the undrained shear strength and D is the pile diameter and

$$p_u = N_p D Su \text{.....................(14)}$$

where

$$N_p = 12 - 4\exp(-\xi d/D) \text{.....................(15)}$$

Where

$$\xi = \begin{cases} 0.25 + 0.05\lambda & \text{for } \lambda < 6 \\ 0.55 & \text{for } \lambda \geq 6 \end{cases} \text{.....................(16)}$$

where

$$\lambda = \frac{Su_0}{d_{su}D} \text{.....................(17)}$$

Where Su_0 is the undrained shear strength at the stop of the soil layer and d_{su} is the rate of increase in Su with depth. The *LAP* input parameters are listed in

$$Ir = \frac{G_{max}}{Su} \text{.....................(18)}$$

Figure 33 shows the normalised from of the Soft clay (Jeanjean) for Ir values of 100, 200, 400, 500, 600 and 700.

Table 9: Parameters for Soft clay (Jeanjean)

Parameter (Units)	Description
Ir (-)	Rigidity index
Su (kPa)	Undrained shear strength at top of soil layer
d_{su} (kPa/m)	Change in undrained shear strength with depth

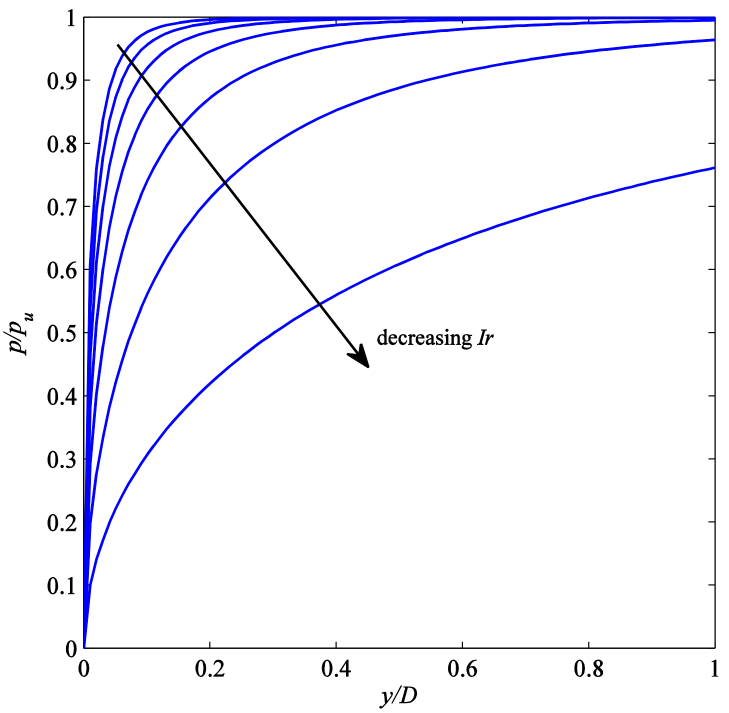

Figure 33: Normalised Soft clay (Jeanjean) p-y curves

Weak rock

The shape of the weak rock PY curve is based on (Reese, 1997) and is made up of three sections. The input parameters that define the curve are given in Table 10 and the general form of the curve is shown in Figure 34.

Table 10: Input parameters for Weak Rock

Parameter (Units)	Description
q_{ur} (kPa)	Compressive strength of rock
α_r	Strength reduction factor
$k_{\underline{\mathrm{rm}}}$ (-)	Dimensionless coefficient in the range of 0.0005 and 0.00005
E_{ir} (kPa)	Initial modulus of the intact rock

The initial (linear) portion of the curve $y \leq y_a$ is given by

$$p = k_{ir}E_{ir}y \tag{19}$$

E_{ir} is an input parameter representing the initial intact modulus of elasticity and k_{ir} is a dimensionless coefficient that accounts for changes in and is given by

$$k_{ir} = \min\begin{cases} 100 + 400\,\dfrac{d}{3D} \\ 500 \end{cases} \tag{20}$$

The limiting displacement for this initial elastic portion y_a is given by

$$y_a = \left(\frac{P_u}{2\;k_{ir}\;E_{ir}\;(k_{rm}D)^{0.25}}\right)^{4/3} \tag{21}$$

where k_{rm} is a dimensionless input parameter that ranges between 0.0005 and 0.00005 and p_u is the ultimate resistance, taken as the minimum of

$$p_u = \min\begin{cases} \alpha_r q_{ur} D\left(1.0 + 1.4\,\dfrac{d}{D}\right) \\ 5.2\alpha_r q_{ur} D \end{cases} \tag{22}$$

The input parameter q_{ur} is compressive strength of the rock. The parameter α_r is to account for the rock fracturing. Reese (1997) suggests adopting taking α_r=1/3 for a Rock Quality Designation (RQD) of 100 and increasing α_r linearly to a maximum of unity for an RQD of zero. The p-y curve for $y \geq y_a$ and $p \leq p_u$ is given by.

$$p = \frac{p_u}{2}\left(\frac{y}{k_{rm}D}\right)^{0.25} \tag{23}$$

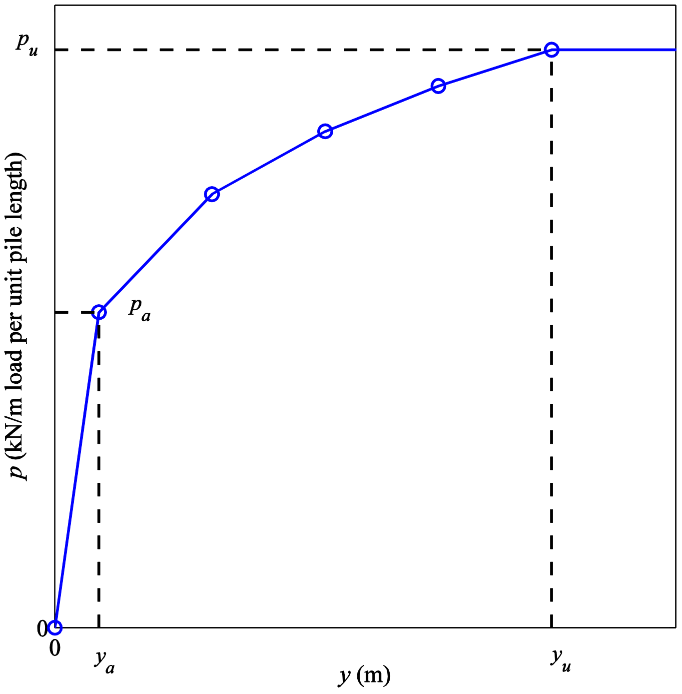

Figure 34: Form of p-y curve for weak rock

Strong Rock

The strong rock *p*-*y* curves are based on (Turner, 2006) and use a tri-linear function illustrated in Figure 35. The ultimate resistance is

$p_u = 0.5Dq_{ucs}$ ....(24)

where qucs is the unconfined compressive strength of the rock. The initial slope is $1000q_{ucs}$ up to $0.8p_u$ or y/D=4E-4. The slope then reduces to $50q_{ucs}$ up to $1.0p_u$. This corresponds to y/D = 2.4E-3. For y/D > 2.4E-3, the slope is zero.

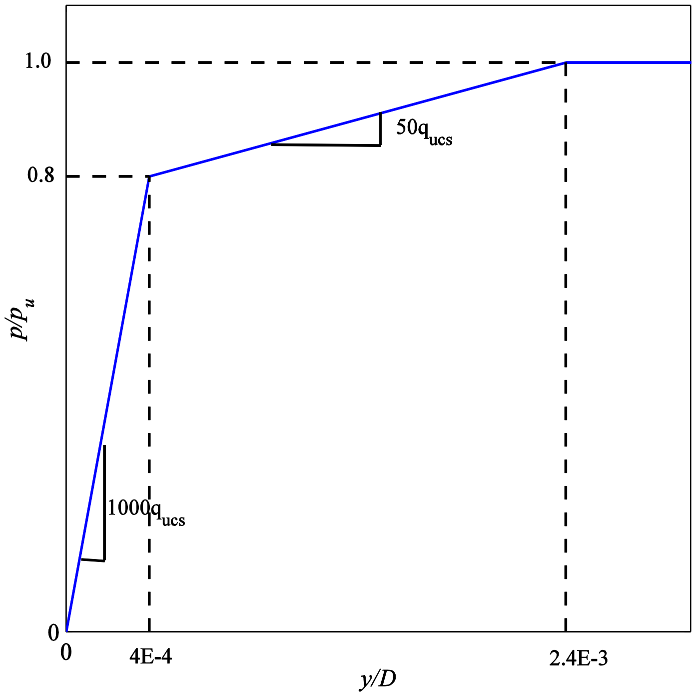

Figure 35: py curve for strong rock

(Turner, 2006) notes that *p*-*y* curves do not account explicitly for rock mass properties, which limits their applicability to massive rock. The authors recommend verification by load testing if deflections exceed 0.04% of the shaft diameter (or $0.8p_u$), which would exceed service limit state criteria in most practical situations. It is recommended that brittle fracture of the rock is assumed be modelled if the *pu* is mobilised. In *LAP*, the *p*-*y* curve has a zero gradient beyond p_u and therefore does not include this “brittle facture” recommendation. Users should therefore check the results of the model in the excel download to ensure that p_u is not mobilised in the model. (Turner, 2006) concludes that the recommended criteria applies only for very small lateral deflections and is not valid for jointed rock masses. The single input parameter for the Strong Rock model is given in Table 11

Table 11: Parameters for strong rock

Parameter (Units)	Description
q_{UCS} (kPa)	Unconfined compression strength

CPT Sand (Suryasentana and Lehane)

(Suryasentana and Lehane, 2014) developed a *p-y* model base the cone penetration test (CPT) end resistance (q_c).

$$\frac{p}{\sigma'_v D} = 2.4\left(\frac{q_c}{\sigma'_v}\right)^{0.67}\left(\frac{d}{D}\right)^{0.75}\left(1 - \exp\left(-6.2\left(\frac{d}{D}\right)^{-1.2}\left(\frac{y}{D}\right)^{0.89}\right)\right) \text{.......................................(25)}$$

For this equation ultimate lateral resistance is

$$p_u = 2.4\sigma'_v D\left(\frac{q_c}{\sigma'_v}\right)^{0.67}\left(\frac{d}{D}\right)^{0.75} \text{...(26)}$$

This can be rearrange to give to investigate the relationship between q_c and the ultimate lateral resistance pressure p_u/D,

$$\frac{p_u}{q_c D} = \left(\frac{q_c}{\sigma'_v}\right)^{-0.33}\left(\frac{d}{D}\right)^{0.75} \text{..(27)}$$

Figure 36 plots the normalised lateral pressure against normalised cone tip resistance for a range of embedment ratios.

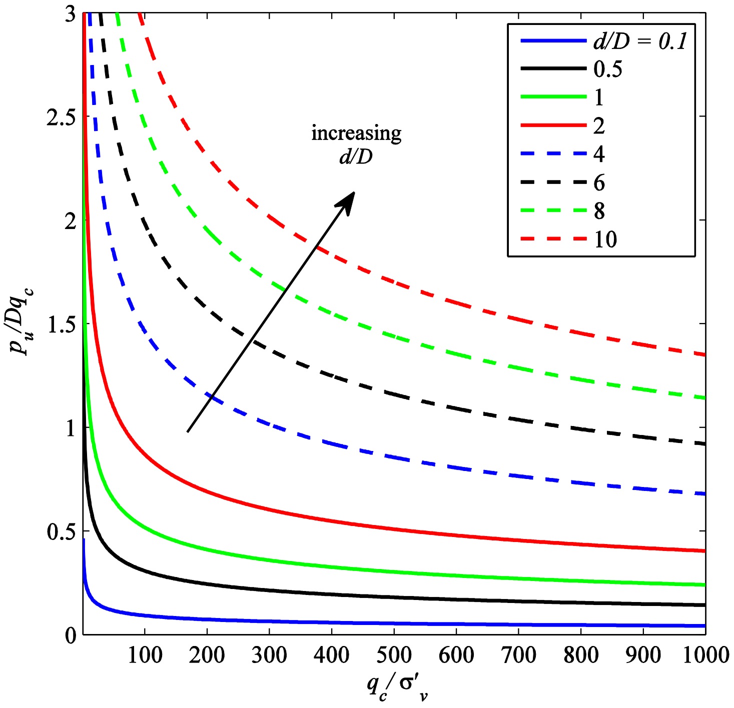

Figure 36: CPT Sand normalised p_u with normalised qc for a range of *d/D* ratios

In the study, q_c/σ'_v ranged between around 450 at a depth of 1m to 100 at a depth of 10m. Assuming a pile diameter of 1m, the p_u/q_cD ratios range between 0.4 at a depth of 1m (d/D=1) and >3 at a depth of 10m (d/D=10).

The normalised displacement required to mobilise the ultimate lateral resistance is plotted in Figure 37 for a range of normalised depths.

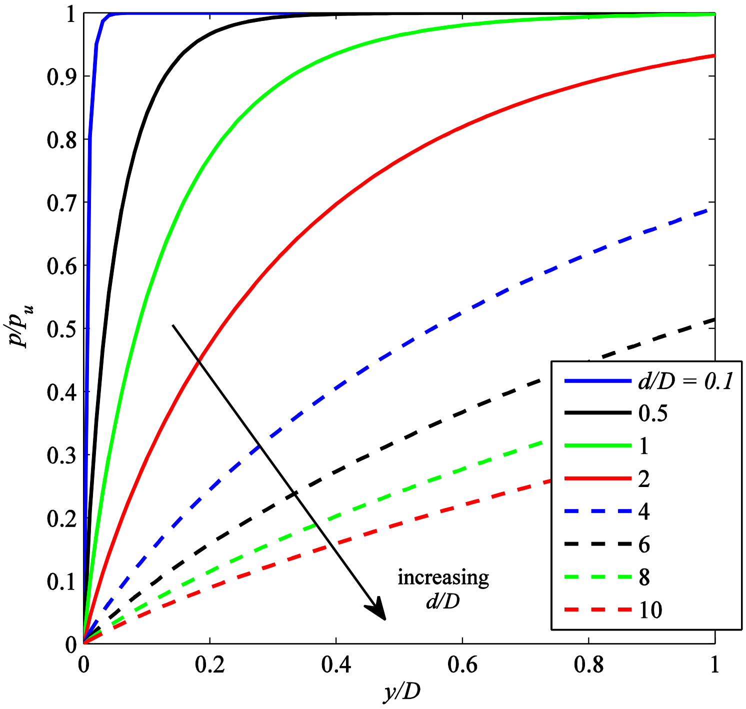

Figure 37: CPT sand normalised *p-y* response

The normalised lateral pressure is plotted against normalised lateral displacement for four values of q_c/σ'_v in Figure 38. In each plot a range of normalised depths are presented. It can be seen that the normalised depth governs the shape of the curve while the normalised cone tip resistance governs the normalised lateral capacity.

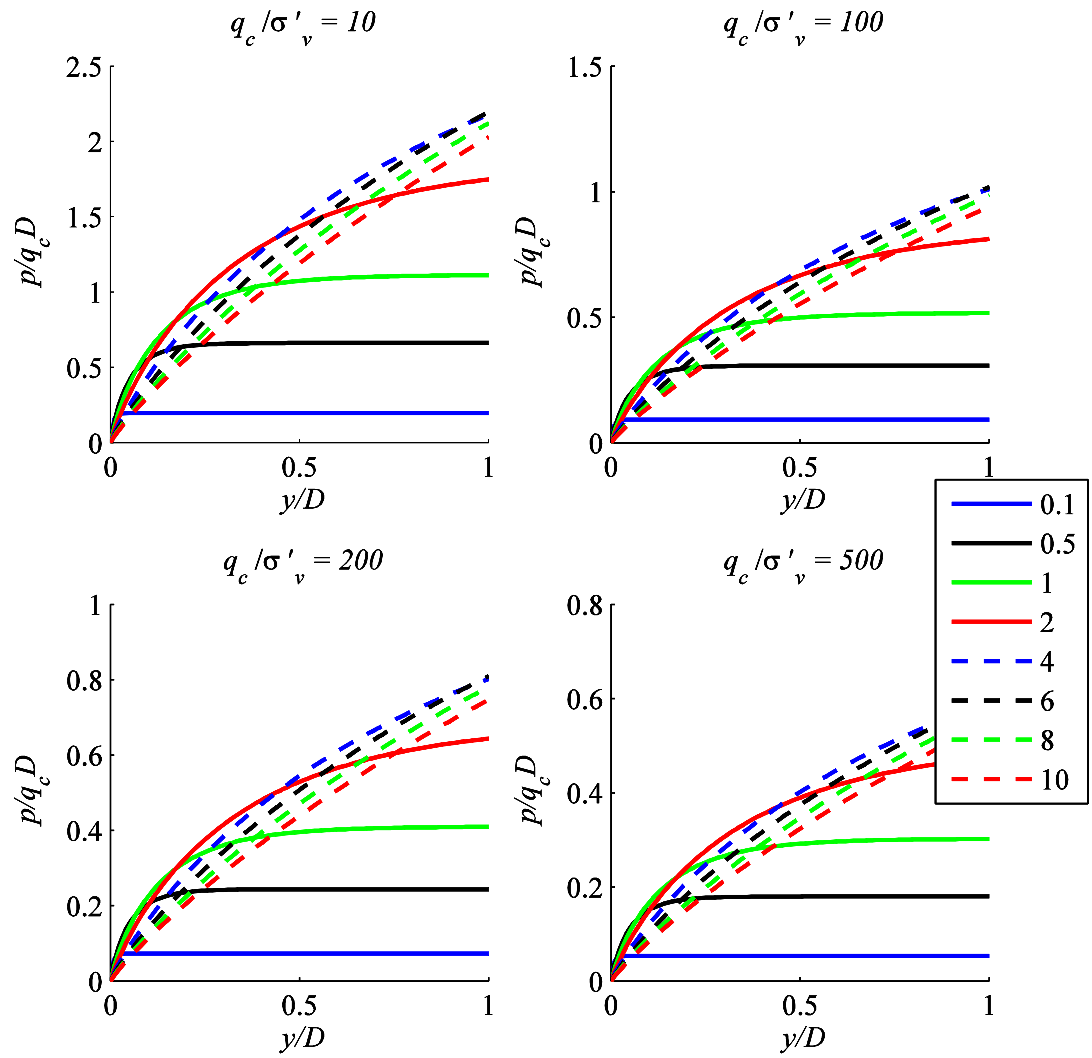

Figure 38: Normalised *p-y* response for a range of normalised qc values and *d/D* ratios

CPT Clay (Truong and Lehane)

For clay soils, (Truong and Lehane, 2014) propose the following relationship between the net cone resistance and the ultimate lateral resistance

$$\frac{p_u}{D} = q_{net}\left(\left(\frac{3}{4.7 + 1.6\ln I_r}\right) + (1.5 - 0.14\ln I_r)\tanh\left(\frac{0.65d}{D}\right)\right) \text{...}(28)$$

Where *Ir* is the rigidity index, *d* is depth below ground surface and *D* is the pile diameter. It can be seen for low *Ir* values and high *d/D* ratios the ultimate lateral resistance exceeds the net cone tip resistance.

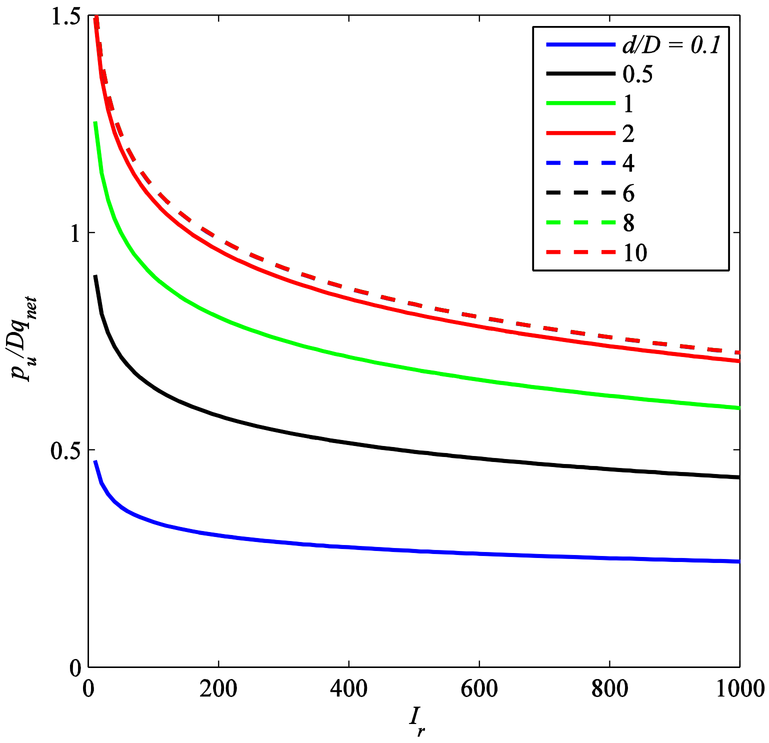

Figure 39: CPT clay py models normalised pu with rigidity index for a range of *d/D* values

The *p-y* curves are then formed using the following equation.

$$\frac{p}{p_u} = \begin{cases} \tanh\left((0.26I_r + 3.98)\left(\frac{y}{D}\right)^{0.85}\left(\frac{d}{D}\right)^{-0.5}\right) \text{ for } \frac{d}{D} < 3 \\ \tanh\left((0.15I_r + 2.3)\left(\frac{y}{D}\right)^{0.85}\right) \text{ for } \frac{d}{D} \geq 3 \end{cases} \text{...}(29)$$

This equation is plotted in Figure 40 for *Ir* = 200 and a range of *d/D* values. Again it can be seen that the curves of *d/D* ≥ 4 are virtually indistinguishable.

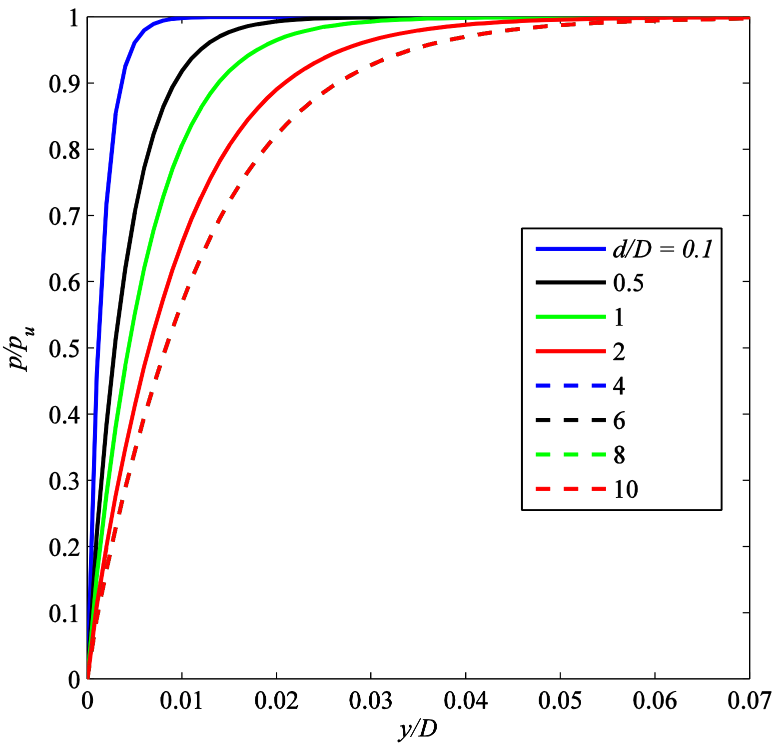

Figure 40: CPT clay normalised *p-y* response for *Ir*=200 and a range of *d/D* values

CPT Carbonate sand (Dyson and Randolph)

(Dyson and Randolph, 2001) developed *p-y* curves for carbonate sands based on the results of a series of model centrifuge tests. The *p-y* curves were developed in terms of CPT q_c measurements and are of the form

$$p = \sigma'_D\, RD \left(\frac{q_c}{\sigma'_D}\right)^n \left(\frac{y}{D}\right)^m \quad \text{...(30)}$$

where σ'_D is the vertical effective stress in the soil one pile diameter below the ground surface. In *LAP*, values of q_c is specified in a table with corresponding depth values. Typically, lower values of *R* are expected at shallow depths (i.e. 1-2 diameters below the ground surface) were surface wedge failure can occur. The value of *R* is therefore defined using a bi-linear function with depth, by specifying the value at the ground surface ($R_{surface}$), the deep value R_d and the depth at which the value of *R* becomes a constant d_R as indicated in Figure 41. The exponents (*n* and *m*) must also be specified. The input parameters for are listed in Table 12.

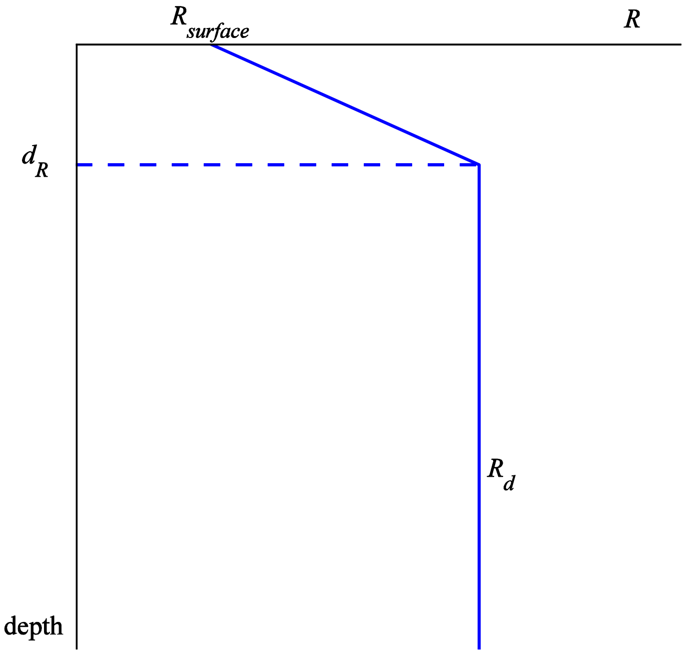

Figure 41: Defining the variation of R with depth for CPT Carbonate (Dyson and Randolph)

.

Table 12: Input parameters for CPT Carbonate Sand (Dyson and Randolph)

Parameter (Units)	Description
$R_{surface}$ (-)	Value of R at surface
Rd (-)	Value of R for d ≥ d_R
dR (m)	Depth after which R is constant
n (-)	exponent
m (-)	exponent
q_c (kPa)	Measured in-situ cone tip resistance
Depth (m)	Depth corresponding to cone measurements

CPT Auto

It also has the option to select “CPT Auto” as a *p-y* type (see Figure 42). The user must then specify if (u2) pore pressure measurements where included (i.e. piezo cone). A method for classifying the soil is then selected. There are four available methods, including the Robertson Fr and Bq methods (Robertson, 1990), the IC method (Robertson, 2009) and the method of (Schneider et al., 2008).

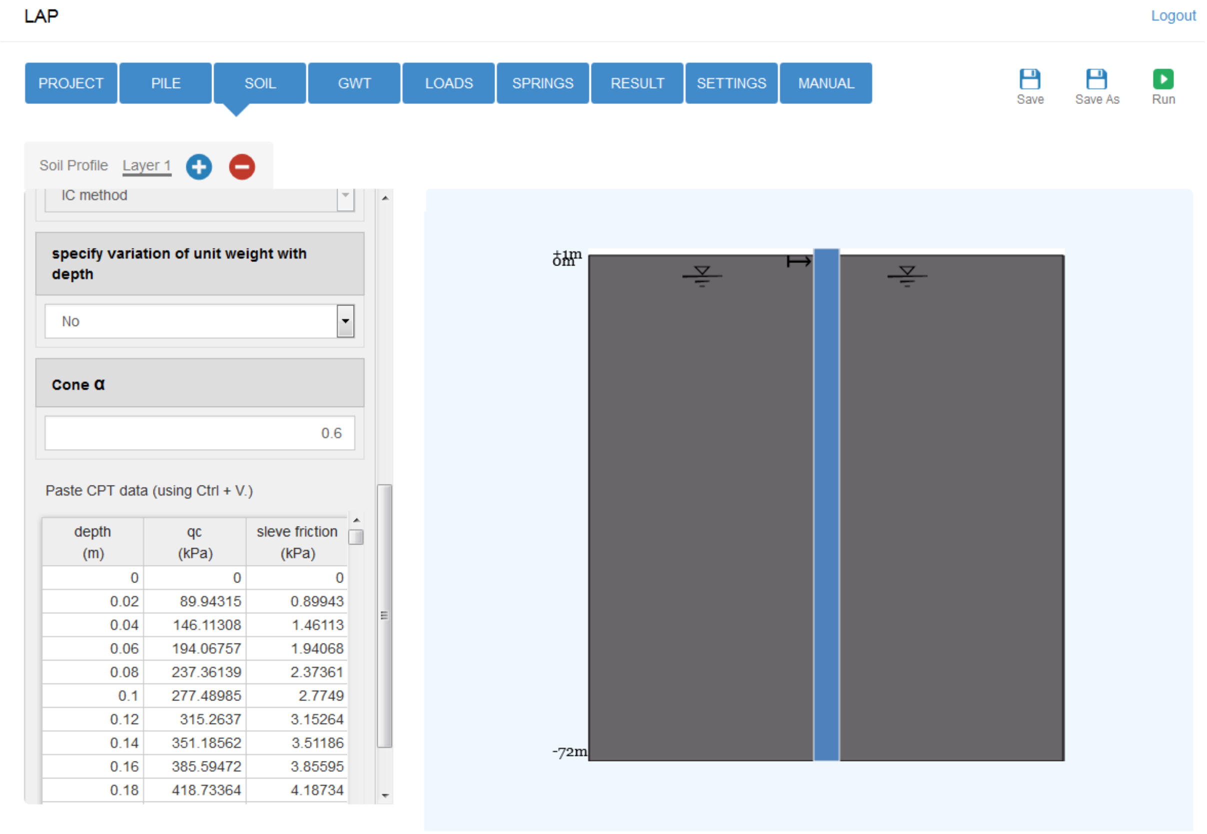

IC method

specify variation of unit weight with depth

No

Cone α

0.6

Paste CPT data (using Ctrl + V.)

depth (m)	qc (kPa)	sleve friction (kPa)
0	0	0
0.02	89.94315	0.89943
0.04	146.11308	1.46113
0.06	194.06757	1.94068
0.08	237.36139	2.37361
0.1	277.48985	2.7749
0.12	315.2637	3.15264
0.14	351.18562	3.51186
0.16	385.59472	3.85595
0.18	418.73364	4.18734

Figure 42: Screen shot from web application of CPT Auto input options

When the analysis is executed, the program first classifies the soil using the CPT data according to one of the selected methods listed above. For example, Figure 43 shows a screen shot from the program where “Robertson Fr” was selected as the classification method. At a particular depth, if the material is classified as a Sand (or a coarser grained material) then, then the *qc* value at that depth is used as an input into Equation (25) (Suryasentana and Lehane (2014)). If the material is classified as a Silt (or a finer grained material) then, then the *qc* value at that depth is used as an input into Equation (29) (Truong and Lehane (2014)).

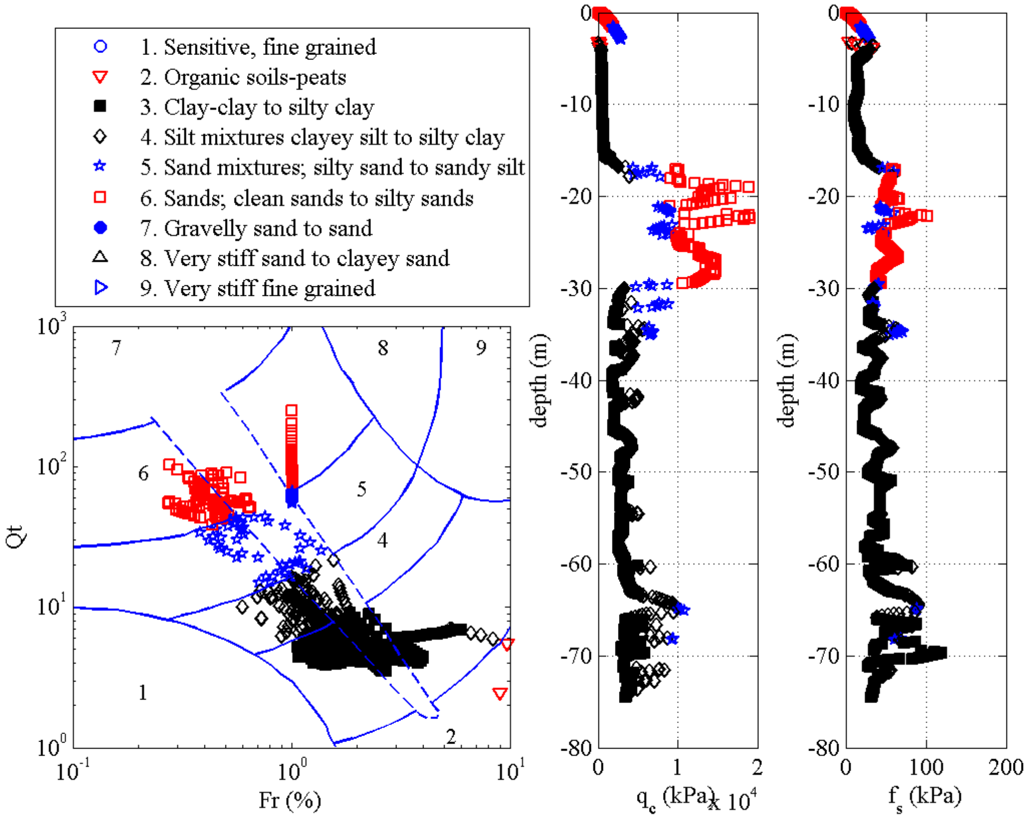

Figure 43: Roberston Fr-Qt classification chart from *LAP*

The ability of *LAP* to use in-situ test data directly as a soil input is unique. While at present the *p-y* curves based on CPT *qc* are considered preliminary and mainly intended for research purposes, in principal, the application requires no engineering judgment to analyse a pile foundation, other than to decide if the CPT data is appropriate for the task. This is likely to lead to more consistent and ultimately more reliable designs (Doherty and Lehane (2016)).

User defined curves

LAP was designed to assist researchers implement and experiment with different *p-y* formulations and contains a particularly convenient method for doing this. Data for *p-y* curves can be assembled in excel by specifying the parameters for the p-y curves with depth (see Figure 44). Seven pre-defined *y* values can be specified (Y1 to Y7) can then be specified at each depth. Seven corresponding *p* values (P1 to P7) can then be computed at each depth using excel formula with the input parameters and corresponding *y* value as input.

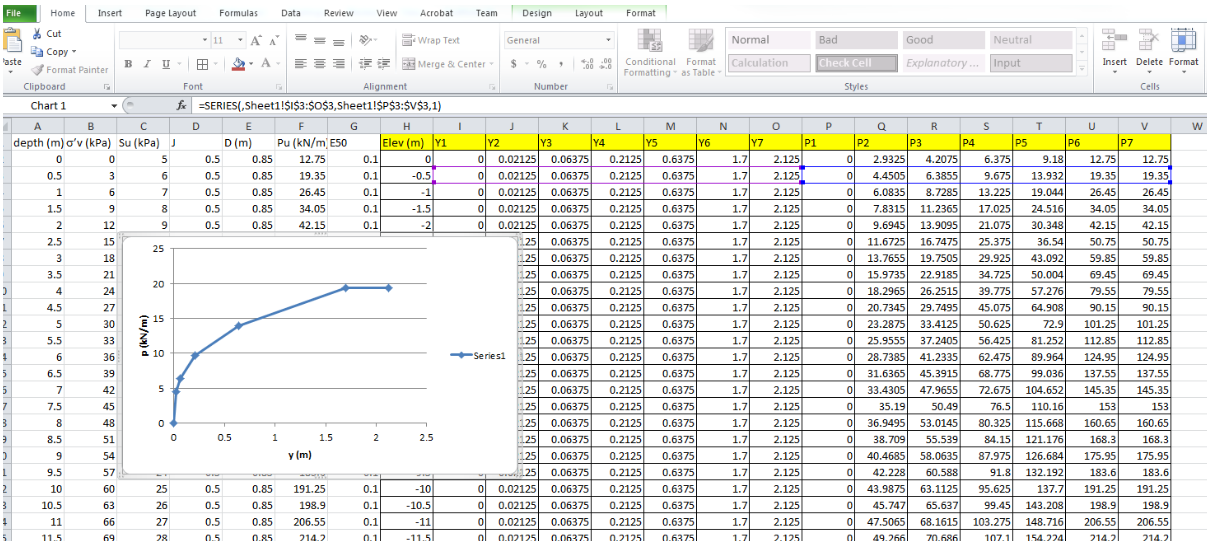

=SERIES(,Sheet1!$I$3:$O$3,Sheet1!$P$3:$V$3,1)

depth (m)	σ'v (kPa)	Su (kPa)	J	D (m)	Pu (kN/m	E50	Elev (m)	Y1	Y2	Y3	Y4	Y5	Y6	Y7	P1	P2	P3	P4	P5	P6	P7
0	0	5	0.5	0.85	12.75	0.1	0	0	0.02125	0.06375	0.2125	0.6375	1.7	2.125	0	2.9325	4.2075	6.375	9.18	12.75	12.75
0.5	3	6	0.5	0.85	19.35	0.1	-0.5	0	0.02125	0.06375	0.2125	0.6375	1.7	2.125	0	4.4505	6.3855	9.675	13.932	19.35	19.35
1	6	7	0.5	0.85	26.45	0.1	-1	0	0.02125	0.06375	0.2125	0.6375	1.7	2.125	0	6.0835	8.7285	13.225	19.044	26.45	26.45
1.5	9	8	0.5	0.85	34.05	0.1	-1.5	0	0.02125	0.06375	0.2125	0.6375	1.7	2.125	0	7.8315	11.2365	17.025	24.516	34.05	34.05
2	12	9	0.5	0.85	42.15	0.1	-2	0	0.02125	0.06375	0.2125	0.6375	1.7	2.125	0	9.6945	13.9095	21.075	30.348	42.15	42.15
2.5	15									0.06375	0.2125	0.6375	1.7	2.125	0	11.6725	16.7475	25.375	36.54	50.75	50.75
3	18									0.06375	0.2125	0.6375	1.7	2.125	0	13.7655	19.7505	29.925	43.092	59.85	59.85
3.5	21									0.06375	0.2125	0.6375	1.7	2.125	0	15.9735	22.9185	34.725	50.004	69.45	69.45
4	24									0.06375	0.2125	0.6375	1.7	2.125	0	18.2965	26.2515	39.775	57.276	79.55	79.55
4.5	27									0.06375	0.2125	0.6375	1.7	2.125	0	20.7345	29.7495	45.075	64.908	90.15	90.15
5	30									0.06375	0.2125	0.6375	1.7	2.125	0	23.2875	33.4125	50.625	72.9	101.25	101.25
5.5	33									0.06375	0.2125	0.6375	1.7	2.125	0	25.9555	37.2405	56.425	81.252	112.85	112.85
6	36									0.06375	0.2125	0.6375	1.7	2.125	0	28.7385	41.2335	62.475	89.964	124.95	124.95
6.5	39									0.06375	0.2125	0.6375	1.7	2.125	0	31.6365	45.3915	68.775	99.036	137.55	137.55
7	42									0.06375	0.2125	0.6375	1.7	2.125	0	33.4305	47.9655	72.675	104.652	145.35	145.35
7.5	45									0.06375	0.2125	0.6375	1.7	2.125	0	35.19	50.49	76.5	110.16	153	153
8	48									0.06375	0.2125	0.6375	1.7	2.125	0	36.9495	53.0145	80.325	115.668	160.65	160.65
8.5	51									0.06375	0.2125	0.6375	1.7	2.125	0	38.709	55.539	84.15	121.176	168.3	168.3
9	54									0.06375	0.2125	0.6375	1.7	2.125	0	40.4685	58.0635	87.975	126.684	175.95	175.95
9.5	57									0.06375	0.2125	0.6375	1.7	2.125	0	42.228	60.588	91.8	132.192	183.6	183.6
10	60	25	0.5	0.85	191.25	0.1	-10	0	0.02125	0.06375	0.2125	0.6375	1.7	2.125	0	43.9875	63.1125	95.625	137.7	191.25	191.25
10.5	63	26	0.5	0.85	198.9	0.1	-10.5	0	0.02125	0.06375	0.2125	0.6375	1.7	2.125	0	45.747	65.637	99.45	143.208	198.9	198.9
11	66	27	0.5	0.85	206.55	0.1	-11	0	0.02125	0.06375	0.2125	0.6375	1.7	2.125	0	47.5065	68.1615	103.275	148.716	206.55	206.55
11.5	69	28	0.5	0.85	214.2	0.1	-11.5	0	0.02125	0.06375	0.2125	0.6375	1.7	2.125	0	49.266	70.686	107.1	154.224	214.2	214.2

Figure 44: screen shot of data assembled in excel with data under the yellow cells pasted into LAP directly

This data can then be pasted directly into *LAP*. Users do not have to worry about ensuring that they define *p-y* data at each node level in *LAP*, as an algorithm is used to find the nearest user specified *p-y* data for each node and then linear interpolation is used over these nearest curves to get an accurate curve at that elevation. A screen shot of the data pasted into *LAP* is shown in Figure 45.

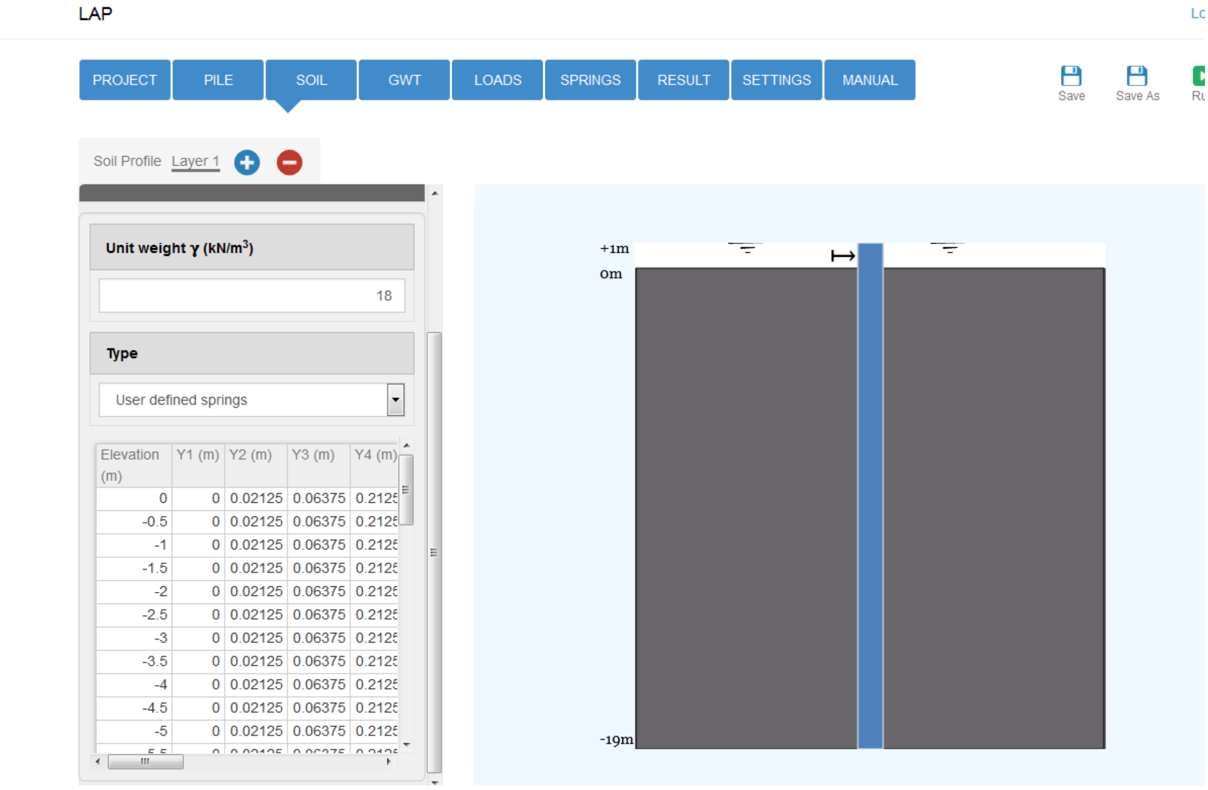

Unit weight γ (kN/m^3): 18

Type: User defined springs

Elevation (m)	Y1 (m)	Y2 (m)	Y3 (m)	Y4 (m)
0	0	0.02125	0.06375	0.2125
-0.5	0	0.02125	0.06375	0.2125
-1	0	0.02125	0.06375	0.2125
-1.5	0	0.02125	0.06375	0.2125
-2	0	0.02125	0.06375	0.2125
-2.5	0	0.02125	0.06375	0.2125
-3	0	0.02125	0.06375	0.2125
-3.5	0	0.02125	0.06375	0.2125
-4	0	0.02125	0.06375	0.2125
-4.5	0	0.02125	0.06375	0.2125
-5	0	0.02125	0.06375	0.2125

Figure 45: screen shot of user specified p-y pasted into LAP

THEORETICAL

Forming the stiffness matrix

LAP uses the finite element method to form and solve systems of non-linear equations representing a vertical pile subjected to lateral loads, displacements, rotations and moments. The pile is represented by a series of 2-noded beam elements. The soil is represented by a series of independent (Winkler) non-linear springs (see Figure 46).

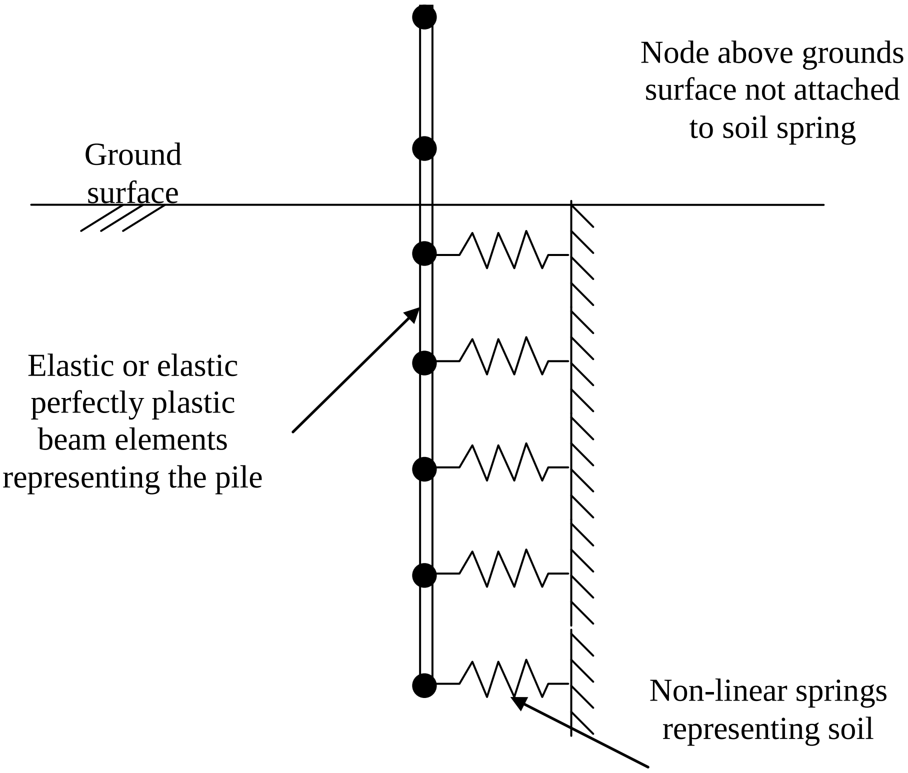

Figure 46: Illustration of beam spring finite element model

LAP works by defining member stiffness matrices for the springs and beams. Each spring has a single degree of freedom, represented by the stretching y_1 of the spring subject to an internal force P_1 (see Figure 47). Internally, compression is taken as positive following convention typically used in soil mechanics. However, with regard to the output *LAP* produces, a positive soil pressure indicates the right hand side of the pile is in compression, while a negative force indicates the left hand side of the pile is in compression with the soil

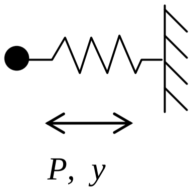

Figure 47: Members stiffness relationship for spring elements

The relationship between the squashing of the spring and the force in the spring is

$P_1 = Ks_1 y_1$ ....(31)

where K_{s1} is the tangent stiffness of spring 1. The member stiffness matrix for a 2-noded beam can be defined in terms of the end rotations (θ_1 and θ_2) subjected to end moments (M_1 and M_2), with clockwise taken as positive (see Figure 48)

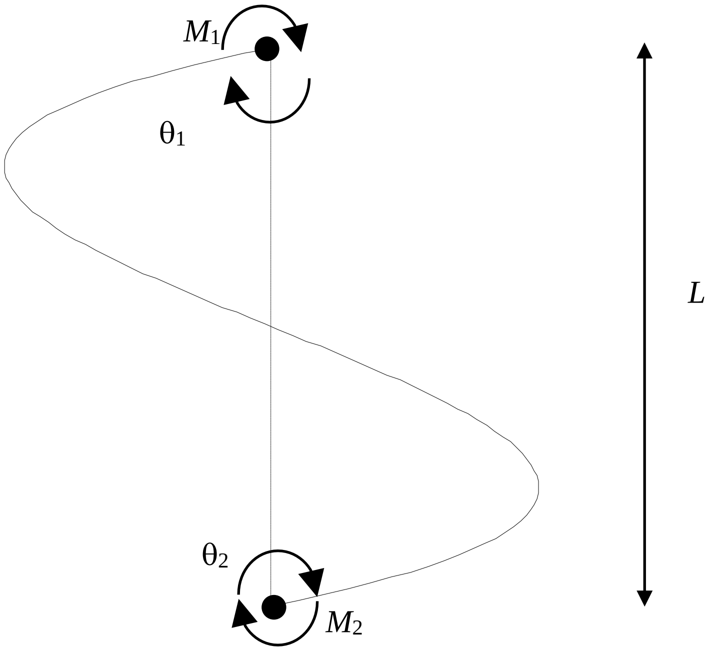

Figure 48: Member stiffness for beam elements

The relationship between end rotations and end moments can be written in matrix form

$$\begin{Bmatrix} M_1 \\ M_2 \end{Bmatrix} = \begin{bmatrix} \frac{4EI}{L^2} & \frac{2EI}{L^2} \\ \frac{2EI}{L^2} & \frac{4EI}{L^2} \end{bmatrix} \begin{Bmatrix} \theta_1 \\ \theta_2 \end{Bmatrix} \quad \text{.......................................(32)}$$

where L is the length of the beam and EI is the flexural stiffness.

A global numbering system for member degrees of freedom is used, as illustrated in Figure 49. Member end rotation are numbered 1 to 2*n* where *n* is the total number of elements. The soil springs are numbers 1 to *j*, where *j* is the total number of nodes below the ground surface.

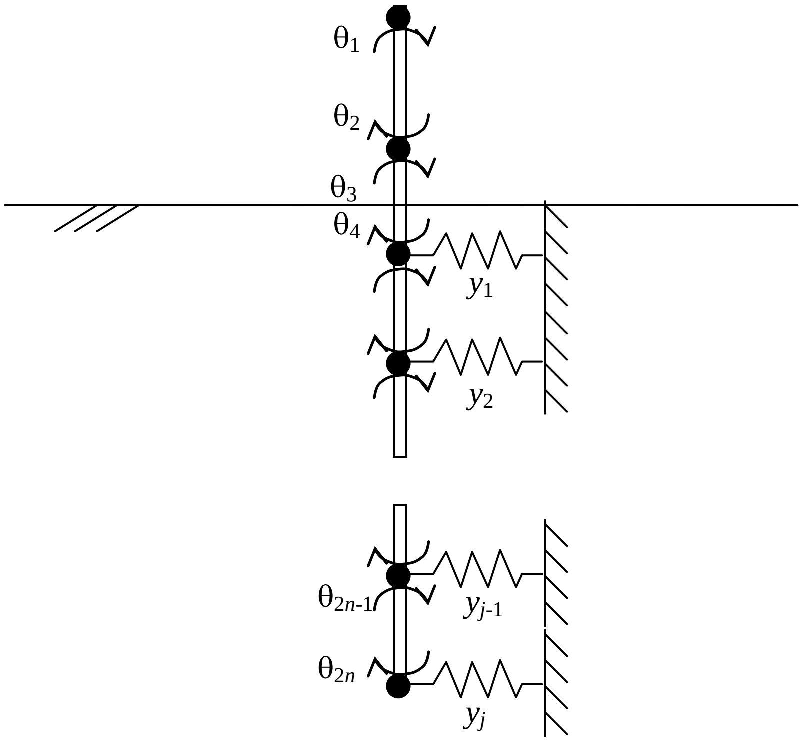

Figure 49: Member degrees of freedom for beam-spring system

A global member stiffness matrix is formed as

$$\begin{Bmatrix} M_1 \\ M_2 \\ M_3 \\ M_4 \\ \cdots \\ M_{2n-1} \\ M_{2n} \\ P_1 \\ P_2 \\ \cdots \\ P_j \end{Bmatrix} = \begin{bmatrix} \frac{4EI_1}{L_1} & \frac{2EI_1}{L_1} & & & & & & & & & \\ \frac{2EI_1}{L_1} & \frac{4EI_1}{L_1} & & & & & & & & & \\ & & \frac{4EI_2}{L_2} & \frac{2EI_2}{L_2} & & & & & & & \\ & & \frac{2EI_2}{L_2} & \frac{4EI_2}{L_2} & & & & & & & \\ & & & & \cdots & & & & & & \\ & & & & & \frac{4EI_n}{L_n} & \frac{2EI_n}{L_n} & & & & \\ & & & & & \frac{2EI_n}{L_n} & \frac{4EI_n}{L_n} & & & & \\ & & & & & & & Ks_1 & & & \\ & & & & & & & & Ks_2 & & \\ & & & & & & & & & \cdots & \\ & & & & & & & & & & Ks_j \end{bmatrix} \begin{Bmatrix} \theta_1 \\ \theta_2 \\ \theta_3 \\ \theta_4 \\ \cdots \\ \theta_{2n-1} \\ \theta_{2n} \\ y_1 \\ y_2 \\ \cdots \\ y_j \end{Bmatrix} \quad (33)$$

This can be written in matrix form

$\{R\} = [K_r]\{r\}$ ....(34)

where $\{R\}$ is a vector of internal actions, $[K_r]$ is the member stiffness matrix for the entire system and $\{r\}$ is a vector of member deformations.

A system of equation is needed in terms of global structural degrees of freedom; with each node having a horizontal displacement and a rotational degree of freedom. A vector $\{u\}$ is used to store these “structural deformation” degrees of freedom and the corresponding “structural actions” (forces and moments) are stored in $\{F\}$. A compatibility matrix $[A]$ is formed that relates structural degrees of freedom to member degrees of freedom as follow

$\{r\} = [A]\{u\}$ ....(35)

The same compatibility matrix can be used to relate internal actions to structural actions

$\{F\} = [A]^T\{R\}$ ....(36)

Combining equations (34), (35) and (36), the relationship between structural degrees of freedom and the structural actions is then

$\{F\} = [A]^T[K_r]\,[A]\{u\}$ ....(37)

By setting the global stiffness matrix

$[K] = [A]^T[K_r]\,[A]$...(38)

Equation (37) can be written as

$\{F\} = [K]\{u\}$ ....(39)

Solution procedure

The global stiffness equation is solved in incremental form, i.e. for the 1st iteration ($j = 1$) of the i^{th} increment

$\{\delta F_i^{\,j}\} + \{F_b^{\,j}\} = [K_i]\{\delta u_i^{\,j}\}$ ....(40)

Where $\{F_b^j\} = 0$ for $j = 1$.With $\{\delta u^j\}$ found, internal actions can be found

$\{R_i^{\,j}\} = \{R_{i\text{-}1}\} + \{\delta R_i^{\,j}\} = \{R_{i\text{-}1}\} + [K_{ri}]\{\delta u_i^{\,j}\}$ ....(41)

$\{R_i^{\,j}\}$ is a vector containing the current internal actions ($\{R_{i\text{-}1}\}$ is the converged solution from the previous increment). The force in each spring is compared with the pre-defined non-linear load displacement response of the spring. The out of balance force $P_b^{\,j}$ at each spring is computed as shown in Figure 50. This force is assembled into an out of balance force vector $\{R_b{}^j\}$.

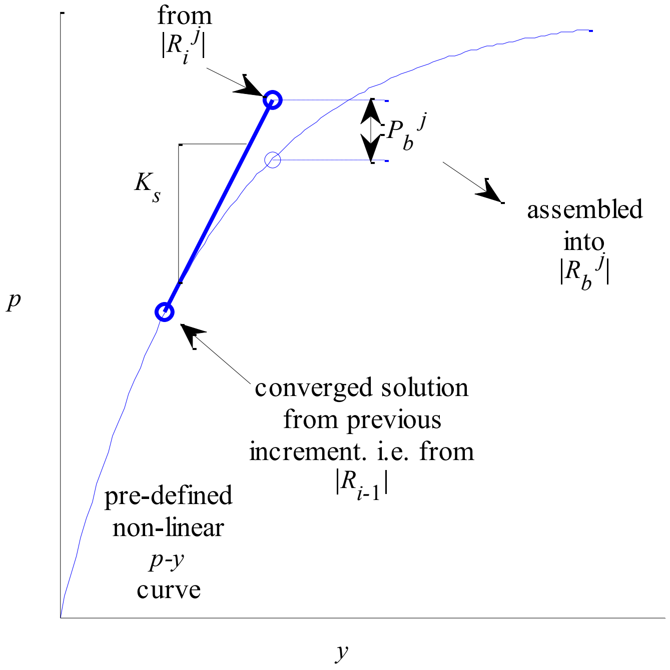

Figure 50: accounting for non-linear springs

Similarly, where elastic-perfectly plastic beam elements are used, the value of the moment at each rotational degree of freedom in $\{R_i{}^j\}$ is compared with the specified plastic moment. If the plastic moment has been exceeded, the value by which the plastic moment has been exceeded is assembled into the appropriate row in $\{R_b{}^j\}$. This out of balance internal force vector is then converted into self-equilibrating structural force vector as follows

$$\{F_b{}^{j+1}\} = [A]^T\{R_b{}^j\} \quad \text{...(42)}$$

The self- equilibrating nature of vector $\{F_b{}^{j+1}\}$ implies that it will not have an impact on the overall equilibrium of the load case. Equation (40) is solved for the next iteration (i.e. $j = j + 1$). This process continues until the maximum relative change in displacement at any node from one iteration to the next is below a specified tolerance. i.e

$$Tol \leq \max\left(\{\{\delta u_i{}^j\} - \{\delta u_i{}^{j-1}\}\}/\{\delta u_i{}^j\}\right) \quad \text{..(43)}$$

and the maximum change in any out of balance force is below a specified tolerance

$$Tol \leq \max\left(\{\{R_b{}^j\} - \{R_b{}^{j-1}\}\}/\{R_b{}^j\}\right) \quad \text{..(44)}$$

By default (see Figure 16), the maximum number of iterations is 1000 (i.e. maximum value for j) and the default tolerance is, tol = 0.005. If the solution fails to converge for any load increment, the magnitude of the load increment is halved and the step is attempted again (i.e. $\{\delta F_i^{\,j}\} = 0.5\{\delta F_i^{\,j}\}$). Three such cut backs are allowed before the analysis is terminated with an error message. By default, the maximum number of steps is 50 (i.e. maximum value for i).

VALIDATION

Outline

This section presents a series is of “test problems” were the results computed by LAP are compared with various analytical solutions to confirm aspects of the model are working as expected.

Validation of Clay (API) static

To valid the accuracy and performance of *LAP*, a model involving a fully embedded 20m long pile in “Soft” API clay was created. The undrained shear strength was assumed to be 10kPa and the ground surface and increase by 2 kPa per metre depth. The total unit weight of the soil was taken as 16k N/m^3 and the water table was assumed to be at the ground surface. The pile as subjected to prescribed displacement of 2 m at the ground surface (see Figure 51).

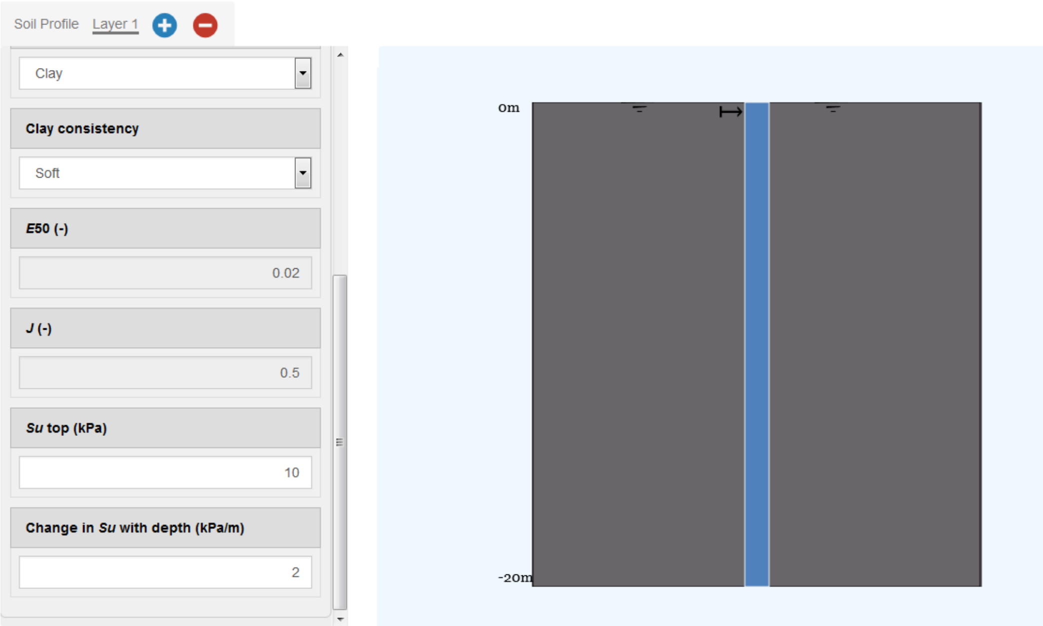

Clay

Clay consistency: Soft

E50 (-): 0.02

J (-): 0.5

Su top (kPa): 10

Change in *Su* with depth (kPa/m): 2

Figure 51: Screen shot of API clay test case

The analysis was conducted with the default solution settings. The following figures use data from the Excel download to examine the performance of LAP. Figure 52 plots the ultimate pressure (p_u) from the Excel download normalised by the elevation specific Su value and Diameter *D* against the elevation. It can be seen that the normalised ultimate pressure ranges between 3 at the ground surface to 9. This is consistent with Equation (10) for API Clay.

The Excel file also contains the p-y response for each node and each load increment in the analysis. Figure 53 shows a comparison of this data with *p* values normalised by p_u and the *y* values normalised by y_c (from Equation (11)). This enables a comparison with the API data from Table 5 at each node for each load increment. It can be seen that the model response matches the expected response.

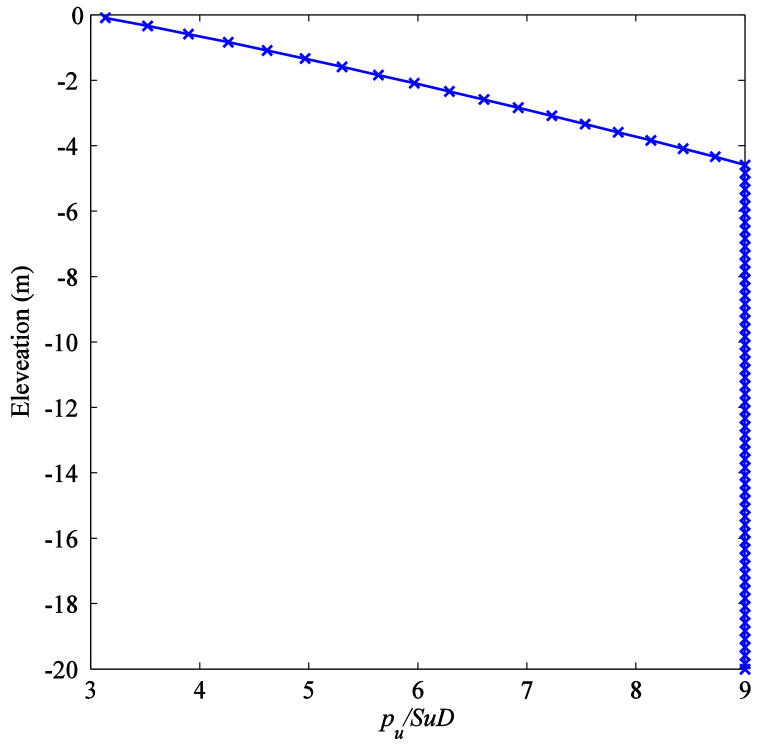

Figure 52: the computed normalised ultimate pressure against elevation

The pressure profile at each load increment is plotted against depth in Figure 54. Also shown are the ultimate pressure profiles (p_u). It can be seen that the pressure profiles lie on or within the ultimate pressure profile.

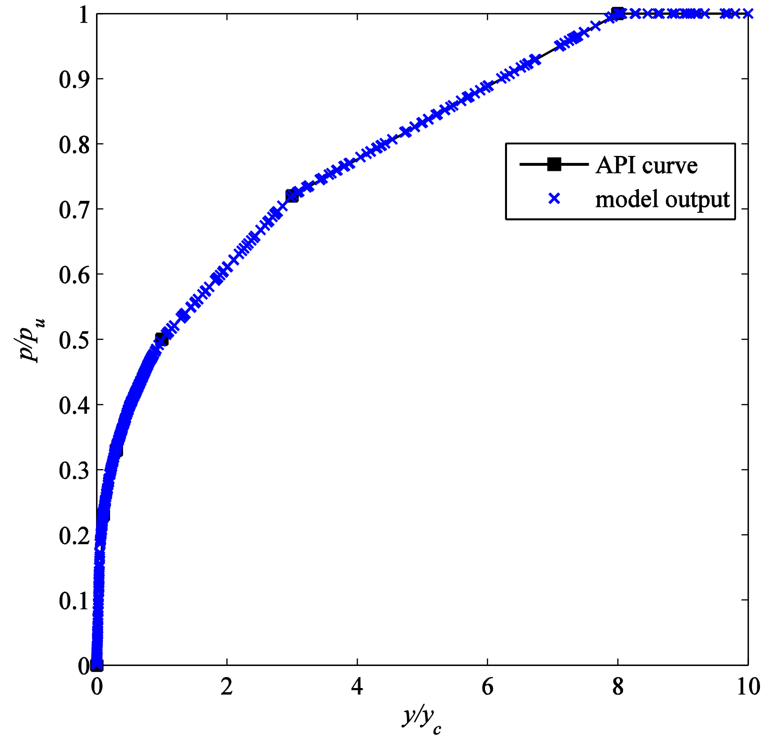

Figure 53: comparison of normalised model response with API curve

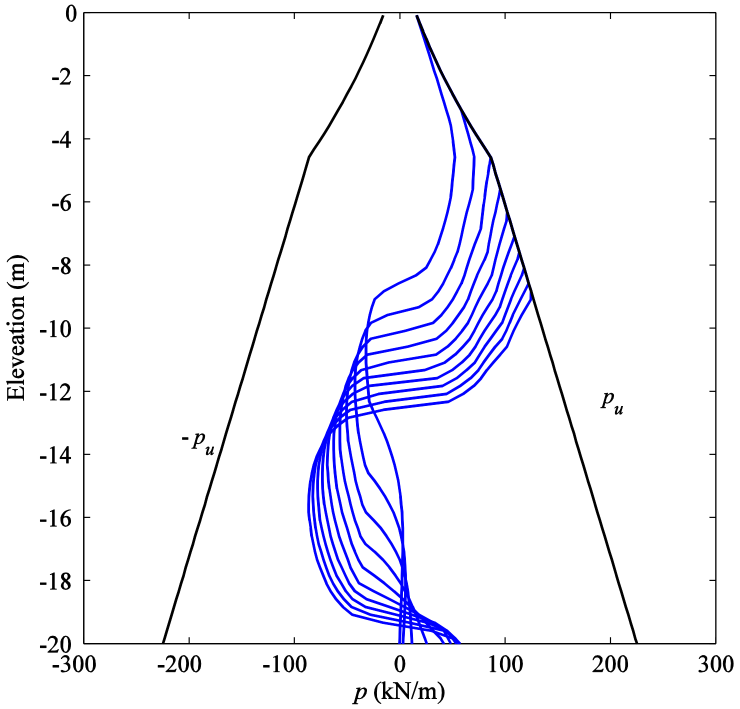

Figure 54: Computed pressure profile at each load increment compare with ultimate pressure

Validation of Clay (API) Cyclic

A problem with the same geometry and boundary conditions (see Figure 51) as that used for the previous example was run with the using the “Cyclic” clay option. Figure 55 shows the computed values of p normalised by p_u and the y values normalised by y_c (from Equation (11)). It can be seen that the softening response of the springs is well captured by *LAP*.

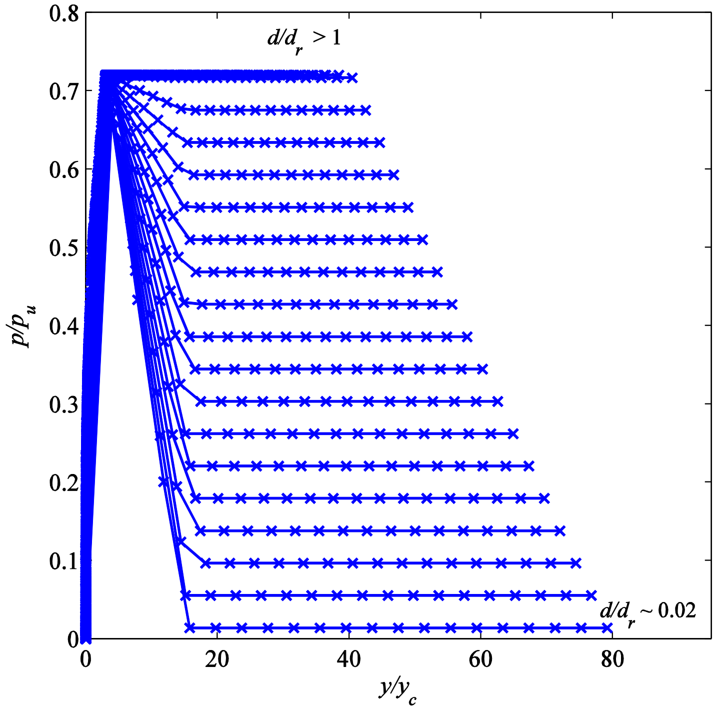

Figure 55: normalised computed py curves for Clay (API) cyclic

Validation of Sand (API)

A problem with the same geometry and boundary conditions (see Figure 51) as that used for the previous example was run with the "API Sand" model using the following soil input parameters; total soil unit weight of 18kN/m^3 and a friction angle of 35 degree. From equations (5), (6) and (7), this results in constants C_1= 2.9704, C_2 = 3.4192 and C_3 = 53.7935. The analysis was run and the ultimate resistance normalised by the vertical effective stress, obtained from the Excel download, is plotted against elevation in. also shown are the relationships from Equation (4). It can be seen that LAP produced the correct ultimate resistance.

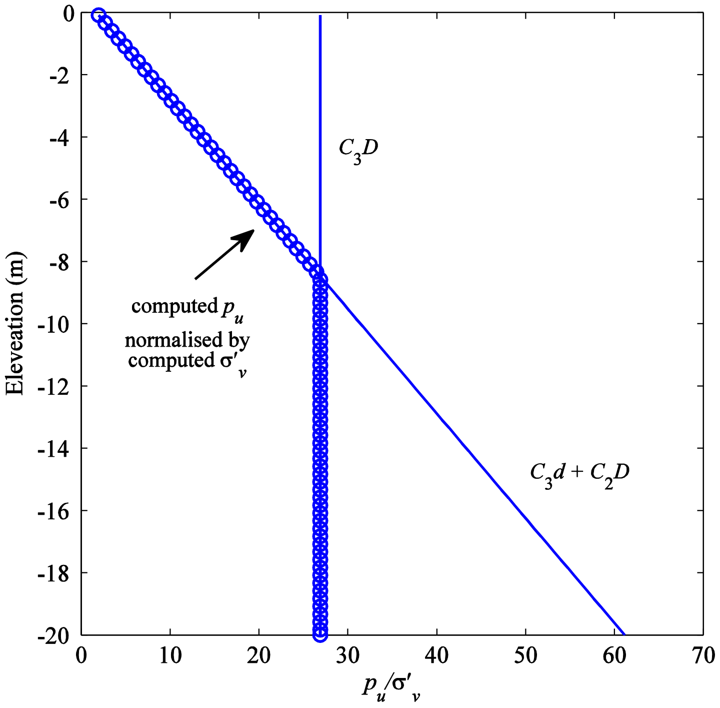

Figure 56: comparison of *LAP* computed p_u and API equations

The p-y response from the excel download was normalised and plotted in Figure 57 for each node and each load increment. It was found that the upper 5 nodes in the LAP model had *A* values (from Equation (9)) that ranged from 2.8667 to 1.2667. The remaining nodes had and A value of 0.9. The analytical p-y curves for API sand (based on Equation (9)) are plotted in Figure 57, were it can be seen that there is very good agreement with the computed response from *LAP*.

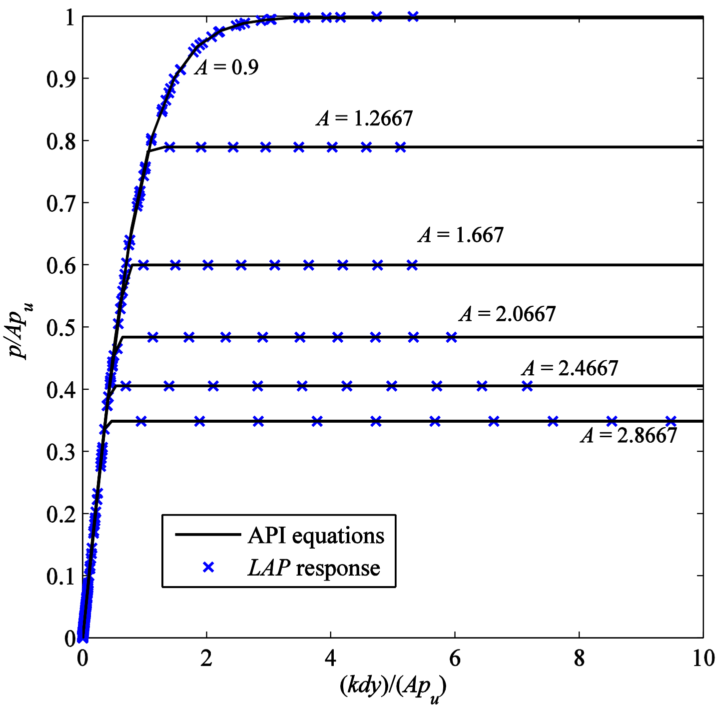

Figure 57: Comparison of LAP computed *p-y* curves for all depth and all load increments with normalised API equations

Elastic behaviour of the pile

A simple cantilever problem was set up such that a pile had a 5 m stick up above the soil, as shown in Figure 58. At the soil surface (i.e. an elevation of 0 m) a prescribed displacement of 0 m was prescribed along with a prescribed rotation of 0 radians. A force (*P*) of 10 kN was applied at the top of the pile. The EI of the pile was specified as 1000 kNm^2. The model there represented a 5 m long cantilever with a point load of 10 kN at the end.

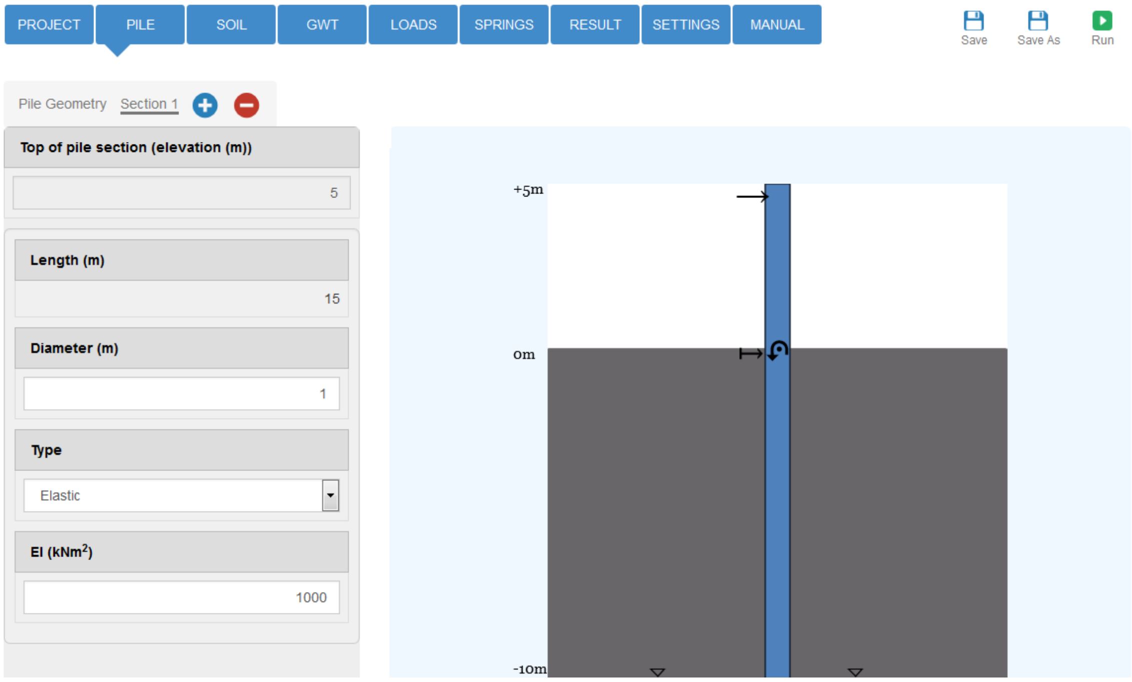

Top of pile section (elevation (m)): 5

Length (m): 15

Diameter (m): 1

Type: Elastic

EI (kNm^2): 1000

Figure 58: Screen shot of pile cantilever problem

The analytical relationship between the force *P* and the defection *u* at end of a cantilever is

$$u = \frac{PL^3}{3EI} \tag{45}$$

Substituting $P = 10$ kN, $L = 5$ m, and $EI = 1000$ kN/m^2 gives $u = 0.41667$ m. This is precisely the magnitude of displacement computed by *LAP* (see the screen shot of pile deflection in Figure 59).

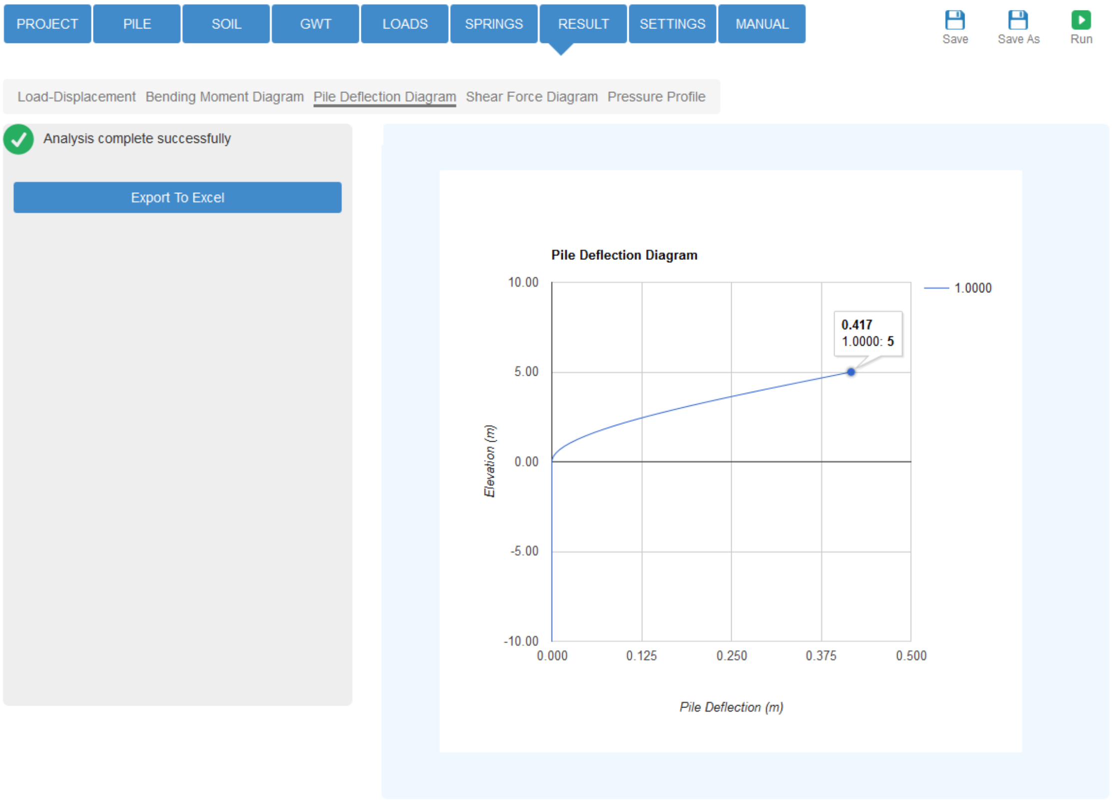

Analysis complete successfully

Figure 59: Screen shot of pile deflection for cantilever problem

Figure 60 shows a screen shot of the load displacement summary plot for the cantilever problem. It can be seen that the load is zero. This is because the load in this summary plot is calculated by summing the forces in the soil springs and any reaction springs (if present). Given that there was no displacement in the pile below the ground surface due to the prescribed displacements, there was zero force in all soil spring.

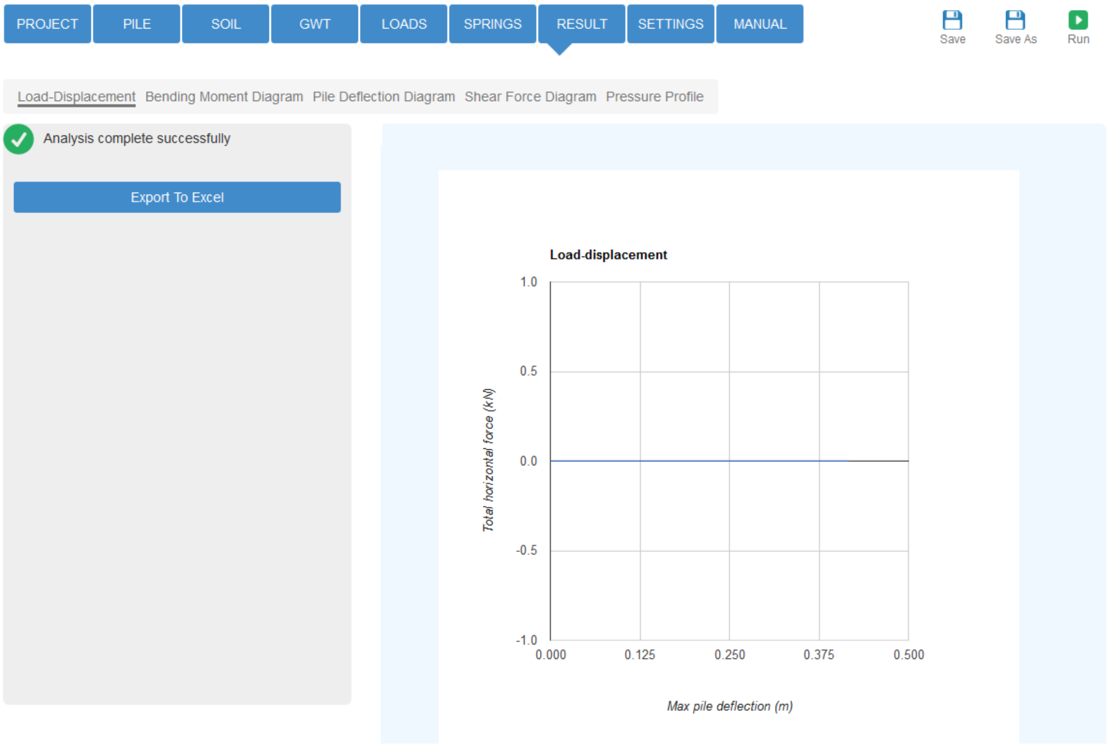

Analysis complete successfully

Figure 60: Screen shot of the Load-displacement summary plot for the cantilever test problem

Elastic perfectly-plastic behaviour of the pile

The same simple cantilever problem was analysed again, but this time using an elastic perfectly-plastic pile with a plastic moment capacity of 30 kNm, as shown in Figure 61.

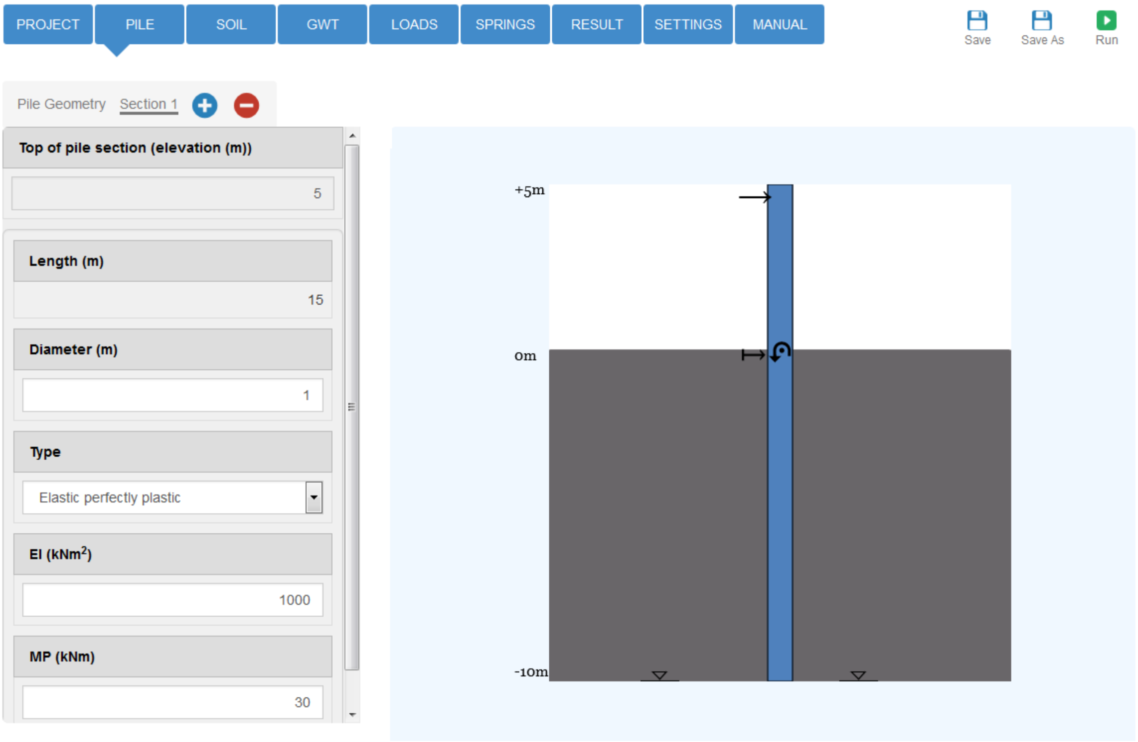

Top of pile section (elevation (m)): 5

Length (m): 15

Diameter (m): 1

Type: Elastic perfectly plastic

EI (kNm^2): 1000

MP (kNm): 30

Figure 61: Cantilever pile with elastic perfectly plastic pile

A screen shot of the results is shown in Figure 62, where a message stating “Analyse failed to convert. Final time step 0.6”. This is expect as the moment at a time step of 0.6 generates a bending moment of 30 kNm in the pile, which is equal to the piles moment capacity. This generate a plastic hinge and a mechanism forms (i.e. collapse).

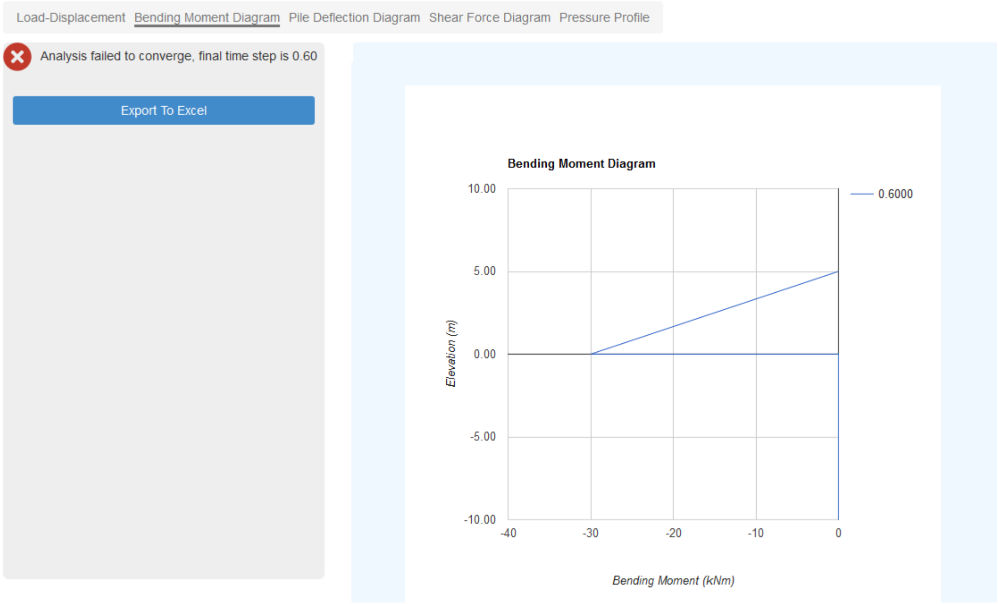

Analysis failed to converge, final time step is 0.60

Figure 62: Results for elastic perfectly plastic pile

REFERENCES

API 2011. Geotechnical and foundation design considerations. Washington DC, USA: American Petroleum Institute Publishing Services.

BRINCH HANSEN, J. 1961. The Ultimate Resistance of Rigid Piles against Transversal Forces. *Geoteknisk Institut,* 12.

DYSON, G. J. & RANDOLPH, M. F. 2001. Monotonic lateral loading of piles in calcareous sand. *Journal of Geotechnical and Geoenvironmental Engineering,* 127**,** 346-352.

JEANJEAN, P. 2009. Re-assessment of P-Y curves from soft clays from centrifuge test and finite element modeling. *Proceedings of the offshore technology conference, paper OTC 20158.* Houston, TX.

MATLOCK, H. 1970. Correlations for Design of Laterally Loaded Piles in Soft Clay. *Proceedings Offshore Technology Conference.* Houston.

O'NEILL, M. W. & MURCHISON, J. M. 1983. An evaluation of p–y relationships in sands. Houston, TX, USA: American Petroleum Institute.

REESE, L. C. 1997. Analysis of Laterally Loaded Piles in Weak Rock. *Journal of Geotechnical and Geoenvironmental Engineering,* 123**,** 1010-1017.

REESE, L. C., COX, W. R. & KOOP, F. D. 1974. Analysis of laterally loaded piles in sand. *Proceedings of the offshore technology conference, paper OTC 2080.* Houston, TX, .

ROBERTSON, P. K. 1990. Soil Classification Using the Cone Penetration Test. *Canadian Geotechnical Journal,* 27**,** 151-158.

ROBERTSON, P. K. 2009. Interpretation of cone penetration tests - a unified approach. *Canadian Geotechnical Journal,* 46**,** 1337-1355.

SCHNEIDER, J. A., RANDOLPH, M. F., MAYNE, P. W. & RAMSEY, N. R. 2008. Analysis of Factors Influencing Soil Classification Using Normalized Piezocone Tip Resistance and Pore Pressure Parameters. *Journal of Geotechnical and Geoenvironmental Engineering,* 134**,** 1569-1586.

SURYASENTANA, S. K. & LEHANE, B. M. 2014. Numerical derivation of CPT-based p–y curves for piles in sand. *Geotechnique,* 64**,** 186-194.

TRUONG, P. & LEHANE, B. M. 2014. Numerically derived CPT-based p-y curves for a soft clay modeled as an elastic perfectly plastic material. *Proc. 3rd International Conference on Cone Penetration Testing, CPT'14.* Las Vegas.

TURNER, J. 2006. Rock-Socketed Shafts for Highway Structure Foundations. *In:* PROGRAM, N. C. H. R. (ed.) *A Synthesis of Highway Practice.* Transportation Research Board of the National Academies.